1992

Centro Svizzero di Calcolo Scientifico

CSCS

Swiss Scientific Computing Center

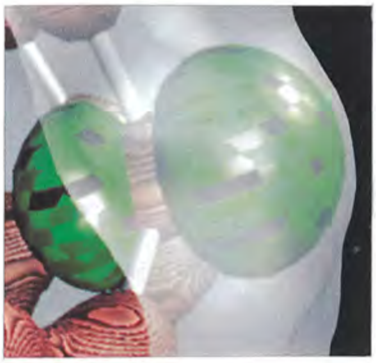

ETH Eidgenössische Technische Hochschule Zürich

Ecole polytechnique fédérale de Zurich
Politecnico federale di Zurigo
Swiss Federal Institute of Technology Zurich

The fullerenes, a new elementary form of carbon, have recently attracted great interest. The figure shows the calculated electronic structure of a hydrogen atom attached to "buckyball" C_{60}, the first discovered representative of this class. Its electron-density is represented by the brown, wood-textured iso-surface (at 0.26 a.u.) which encloses each pair of atoms connected by a double-bond within one lobe (notice that one double-bond has been broken by the attached muon). The semi-transparent grey surface is also an iso-electron-density surface, but at the lower value of 0.01 a.u., forming an outer envelope (with a bump above the muon) as well as an inner cavity. The green surface with a chessboard pattern represents the spin-density at 0.01 a.u. which is essentially located at the nearest neighbor of the muonated C-atom. The spin-density distribution determines the hyperfine interaction which is experimentally accessible by muon spin spectroscopy. In these experiments, also performed at PSI, positive muons (light pseudo-isotopes of H) are used to investigate the microscopic structure of these new materials. The ab-initio geometry optimization and the electronic structure calculation have been performed on the NEC SX-3 (D. Maric) and the visualization on a Silicon Graphics VGX workstation using the MOLEKEL-package (P. Flükiger).

Investing in the Future

The mission of CSCS is the creation and distribution of knowledge to stimulate technological progress and economic success. CSCS high-performance computing offers solutions to academic, business, environmental and human problems.

CSCS means leadership for the future.

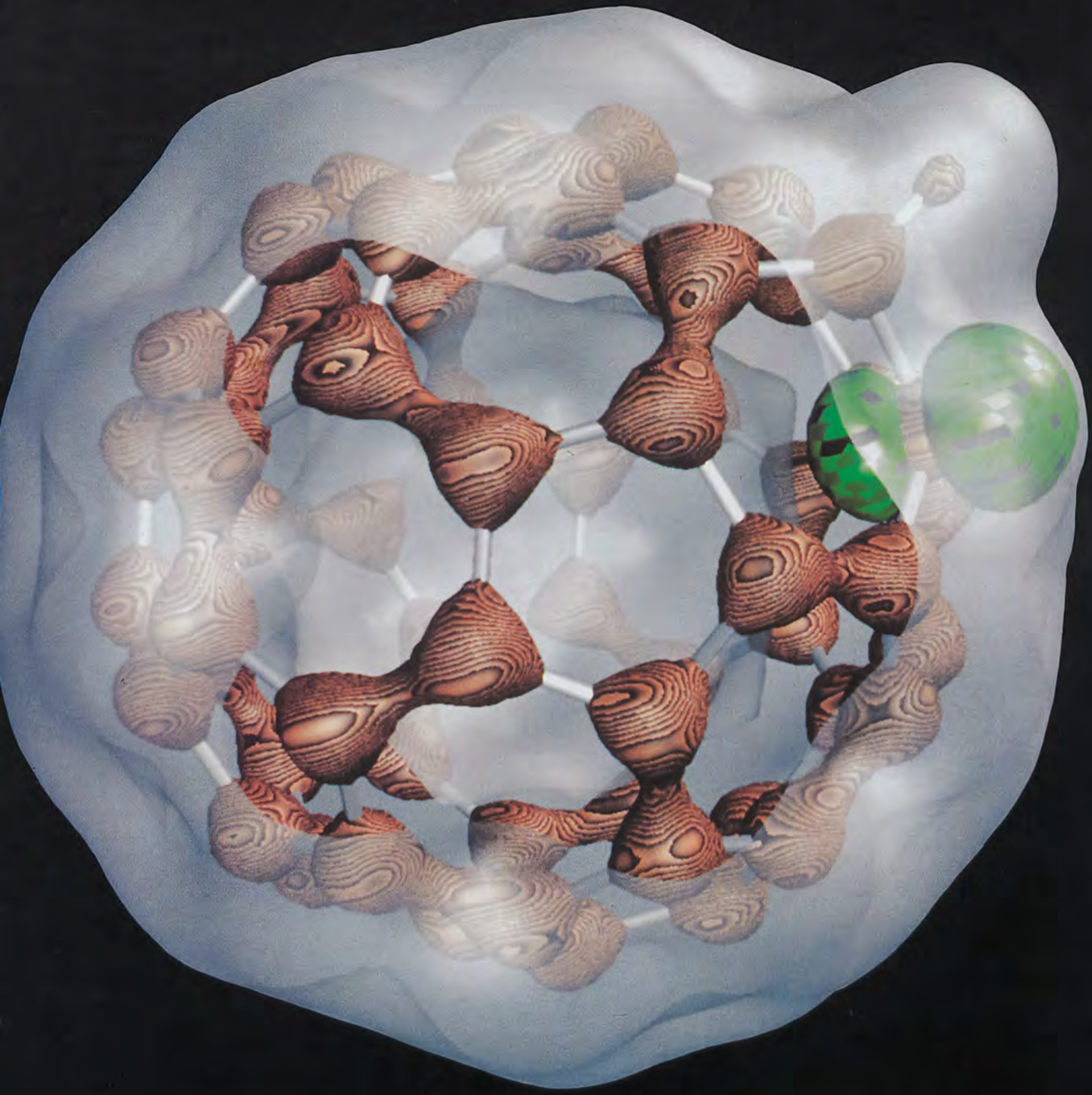

CSCS 1992

Published 1993.
Printed in Switzerland

Centro Svizzero di Calcolo Scientifico (CSCS), also known as the Swiss Scientific Computing Center, Via Cantonale, 6928 Manno, Switzerland. CSCS is affiliated with the Eidgenössische Technische Hochschule Zürich (ETHZ), also known as the Swiss Federal Institute of Technology Zürich.

All financial aspects of CSCS are under the direction of ETH Zürich.

Photography by Franco Mattei, 6702 Claro, Switzerland.

Printed by Fratelli Roda SA, Industria grafica e cartotecnica, 6807 Taverne, Switzerland.

Table of Contents

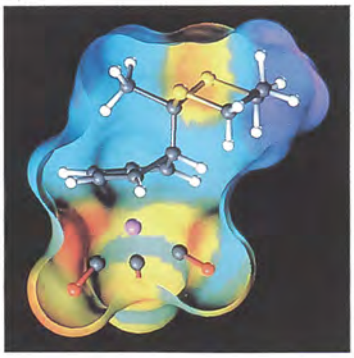


NEC
SX-3
model 22
NEC
SX-3
model 22

Preface

The Centro Svizzero di Calcolo Scientifico (CSCS) has the responsibility to provide Swiss scientists and engineers with the computational resources needed to solve interdisciplinary scientific problems. CSCS users represent various disciplines: physics, chemistry, biology, environmental sciences as well as various engineering disciplines. They come also from many different universities, research institutes and federal technology institutes.

CSCS offers both state-of-the-art computer facilities and high-performance graphics facilities for advanced computer simulations, as well as world class expertise. CSCS remains on the leading edge by continually evaluating technological developments for potential benefits. The center is proud to provide technical leadership, facilities and infrastructure for application-driven research in computational science.

It is recognized today that simple technology transfer (e.g., installing hardware or software) is ineffective unless users are educated and trained properly. The CSCS team of experts plays an important role in this knowledge transfer by educating and training a new generation of scientists and engineers familiar with both scientific problem solving and high-performance computing.

To successfully compete in the future, a combined effort of government, academia and industry is necessary to coordinate interdisciplinary research, create industrial consortia and lead collaborative R&D projects. Additionally, CSCS strives to increase public awareness and understanding of the societal benefits to be gained through advanced computing.

CSCS only recently joined the computational science community and is proud of its innovative attributes: creativity, assertiveness and courage. Combined with expertise and leading edge technology, these attributes provide CSCS with a dynamic environment and a productive atmosphere.

Prof. Dr. R. Hütter

Eidgenössische Technische
Hochschule Zürich
Switzerland

Dr. A. Scheidegger

Centro Svizzero di Calcolo Scientifico
Manno, Switzerland

Overview

Background

The Centro Svizzero di Calcolo Scientifico (CSCS) is the national scientific computing center in Switzerland. The center hosts the most powerful high-performance computer resources currently available for problem solving. The success of the center has been due to a close partnership and support of the Swiss Federal Institute of Technology Zürich and several steering committees and boards. In particular, the CSCS Council advises on the strategic development of the center , and the CSCS Committee, based on scientific criteria, proposes computing resource allocation and distribution, and supervises aspects of technical operation.

The history of CSCS begins in the mid 1980's. The Swiss government empowered a special task force to study the discipline of computer science; this study resulted in a clearly defined goal and comprehensive plan to promote computer science in education and research and its application in industry.

One part of this plan was the procurement of a high-performance, latest generation computer as a national resource. The responsibility of managing, operating and maintaining this national resource was given to the Swiss Federal Institute of Technology Zürich. After extensive evaluation, the Nippon Electric Corporation (NEC) SX-3 was selected as the appropriate vector computer to fulfill Switzerland's high performance computer needs. A site near Lugano was chosen for locating the center.

The computer, installed in a new building at the end of 1991, commenced production in May 1992. CSCS was officially inaugurated on October 1, 1992.

During this past year, CSCS has developed into a reliable and valuable computational service center. The evaluation and acquisition of additional service resources, such as high-speed networking and automatic file-serving facilities further propelled its capabilities.

Several high-performance computing training courses addressing the special needs of computation intensive research are offered to professionals and students. These courses were conducted through a joint effort of CSCS and NEC staff. The quarterly *Crosscuts* newsletter keeps users up-to-date. CSCS also is home to the Speedup, a society which biannually brings together high-performance computer users and publishes a journal based on these meetings. The center has a computer science reference library with a connection to the ETHICS interlibrary service.

All CSCS activities reflect the dedication to user support. The organizational structure is streamlined, based on tasks and information flow, in a further effort to serve the users. User support and satisfaction is the primary and ultimate objective of CSCS.

CSCS Facilities: A Hardware Profile

CSCS provides access to the fastest computer resources for numerical experimentation, data handling and visualization.

Computing power. The available high-performance vector computer is a NEC SX-3 two-processor model with 2 GBytes of main memory and 4 GBytes of extended memory. The SX-3 carries the concept of parallel processing far beyond that of other vector computers. Sixteen vector arithmetic pipelines result in a potential speed of 5.5 Gflops at a clock cycle of 2.9 ns. A computing power upgrade is foreseen in the middle of 1993.

File-serving and archiving. A high-speed, large-capacity file server and archival file-storage system is an essential component for large data handling. To meet this demand, a Convex system with Unitree file management software was installed in early 1993. The initial archiving capacity is 1.8 TB and shall be systematically enlarged to 3 x 70 TB. For file-serving, RAID-Disks will be installed.

Scalable parallel computer systems. Application and productive utilization of parallel distributed computing systems is a new and exciting realm. CSCS is working hard to expand its expertise base in this area in order to offer these facilities to scientists and engineers. Hardware platforms (such as a Meiko Computing Surface) will be installed in early 1993 as a tool for R&D efforts, education and postgraduate training.

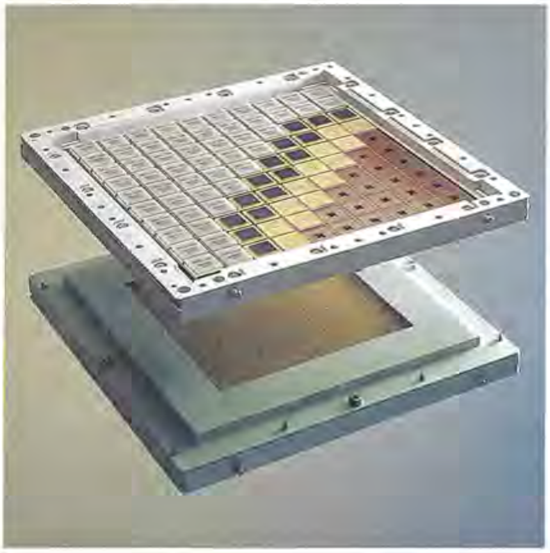

High-Speed Networking

The network concept is continually under development in cooperation with the Swiss education and research network SWITCH. Fault-tolerant remote access to CSCS facilities is guaranteed via the 2 Mbit/s backbone quadrangle Zürich-CSCS-Lausanne-Bern-Zürich. An upgrade is being studied.

Locally, a double FDDI ring enables large-scale data transfers. CSCS presently is involved in the development of high-speed networking using Gbit/s communication links with security as a prime consideration. Central to this effort is the High-Performance Parallel Interface (HiPPI) that operates at 0.8 Gbit/s. HiPPI links will be connected by a central 32 x 32 crossbar switch (PS-32) from Network Systems Corporation (NSC). The figure shows the desired configuration.

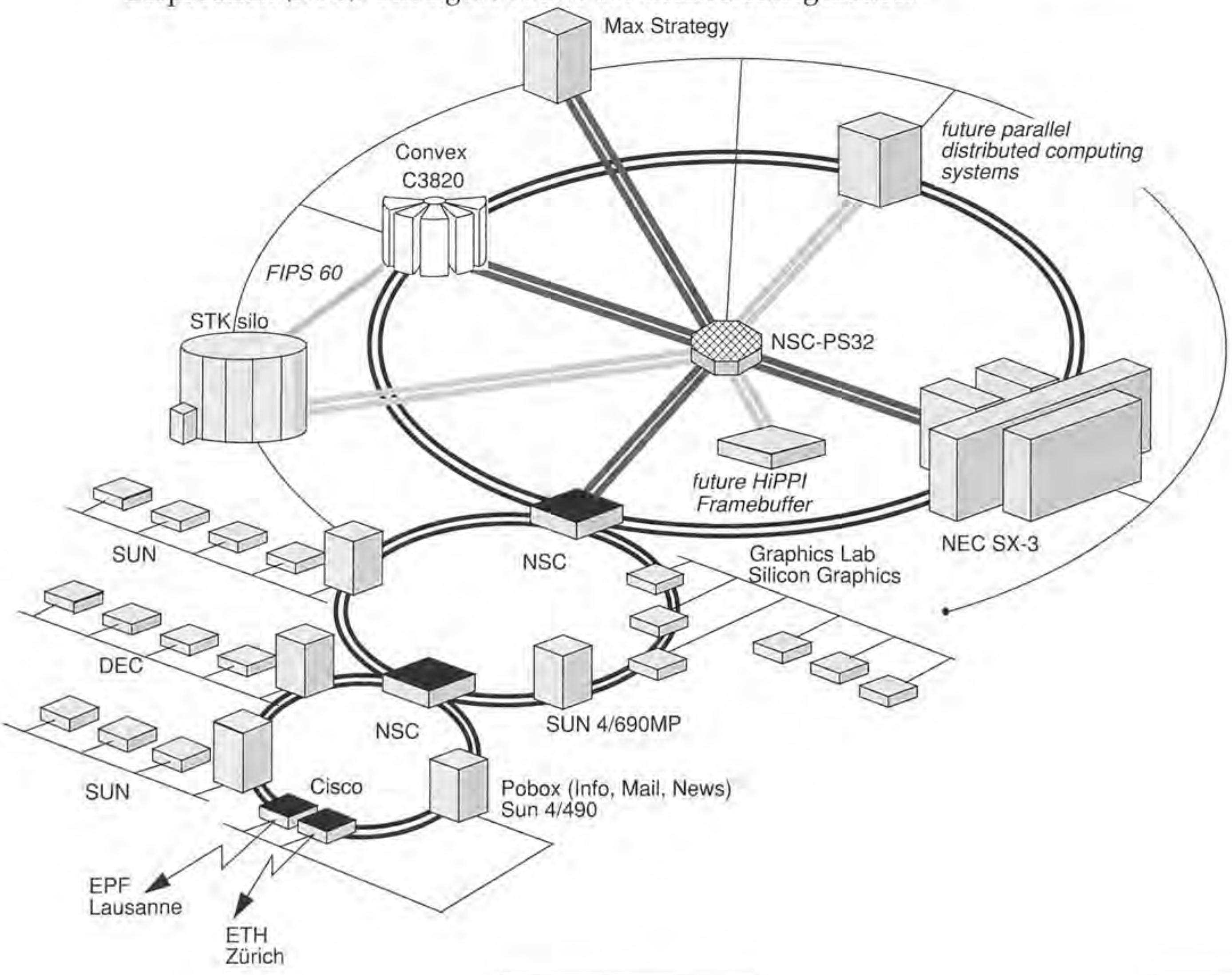

Scientific Applications

Scientific application support and consulting are offered to users of CSCS. Our application software support specialists cover a wide range of disciplines and offer the best expertise for porting, optimizing and adapting user programs to run most efficiently on the specific CSCS computer architecture. CSCS experts support usage of a variety of packages such as:

Mathematical Libraries

ASL	Advanced Scientific Library from NEC
MATHLIB	NEC Mathematical Library
NAG	General Mathematical Library
BLAS	Basic Linear Algebra Subprograms, Levels 1,2 and 3
EISPACK	Matrix Eigenvalue Problem Solver
LINPACK	Linear Algebra Subroutine Library
MINPACK	Nonlinear Optimization Package
LAPACK	Linear Algebra Routines Successor to Linpack and Eispack

Scientific Software

AMBER	Molecular Mechanics and Dynamics
AMOSS	Large-Scale Electronic Structure Calculations
DYNA3D	Structure Analysis and Crash Simulation
GAUSSIAN	Ab initio Electronic Structure Calculations
TASCFLOW	3-D Computational Fluid Dynamics Package

Visualisation

AVS	Interactive Modular Visualisation Package
IRIS EXPLORER	Interactive Modular Visualisation Package
PW-WAVE	Data Analysis and Visualisation Software
MOLEKEL	Molecular Visualisation Program

Recent experience showed that improved user codes for the vector units of the NEC SX-3 results in increased computational capabilities of high-performance computing. CSCS specialists, with the assistance of the on-site NEC team of specialists, rewrote parts of programs, replaced algorithms and reorganized data structures.

Today, the new world of high-performance computing with parallel machines is emerging. The challenge is to develop software environments to ease the use of these machines through the development of new parallel algorithms and applications. Anticipating these needs, CSCS already has built up a new research and development team in parallel computing.

Graphics and Visualization

Visualization is of paramount importance when dealing with large and complex numerical results. CSCS provides the user with a rich graphics environment: combining state-of-the-art hardware and software to allow scientists and engineers to explore their data. High-end graphics workstations are accessible for visualization, for high-performance, interactive, three-dimensional image rendering, and for developing and tuning graphics applications. A video recording facility, as well as color output on paper or transparencies, also are available.

The installation of several professional visualization packages has addressed most user needs; local CSCS modifications and extensions have increased the capabilities of some packages.

Another aspect of visualization activity in CSCS is interactive image synthesis and the processing on innovative computer architectures. Increasingly it is necessary to utilize distributed computers that have the required power, memory capacity and bandwidth. Indeed visualization is computationally demanding, yet the advent of color workstations with accelerated graphics is enabling scientists to investigate their findings more rapidly and convincingly.

Industrial and Commercial High-Performance Computing

Cooperation with the private sector promotes high-performance computing techniques in industrial R&D and commercial enterprises.

Cooperative projects between CSCS and industry focus on knowledge and technology transfer which ultimately bring about technological advances. CSCS offers industry and commercial enterprises the same quality service and resources as universities: access to top specialists, advanced computer hardware, software, networks, storage devices and visualization tools. In addition, CSCS offers integrated solutions for industrial and commercial problems.

A product-oriented and market-driven industrial or commercial enterprise, paired with the technical and scientific expertise of CSCS, undoubtedly is a formula for success.

Who Uses CSCS?

The primary users of CSCS computing resources are Swiss universities, the two federal institutes of technology, and the federal research institutes.

Ninety percent of the available computing time is consumed by large scale projects; the remaining ten percent is divided among approximately 100 users with small and medium size projects. (A medium size project is one requiring less than ten CPU hours per month).

Relevant application fields include: physics, chemistry, biology, engineering and environmental studies. The scientific publications of CSCS users in these application fields are numerous and can be reviewed in Chapter 10.

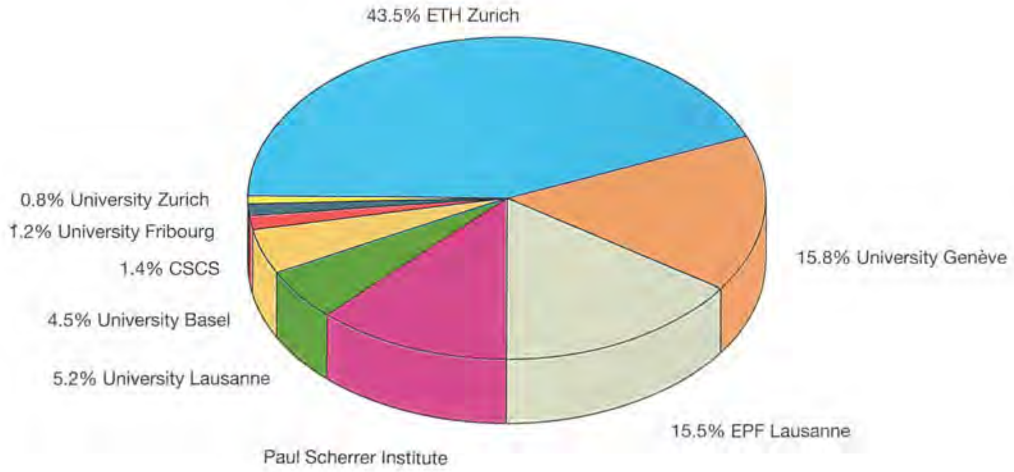

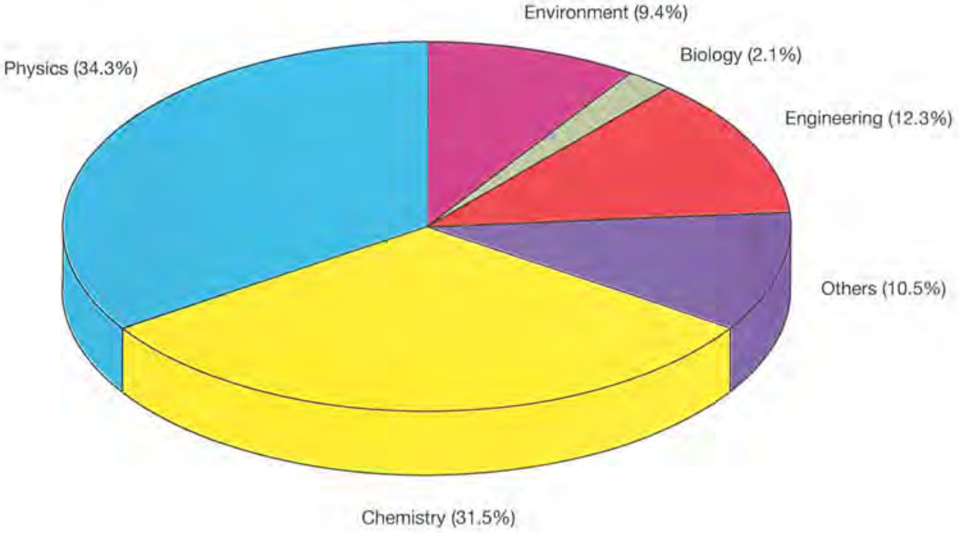

CSCS Projects

Large scale projects registered for 1992

Biology

"Struktur und Dynamik von Proteinen"
Dr. W. Braun, Inst. für Molekularbiologie und Biophysik, ETHZ

"Computer simulation and theoretical chemical studies of the catalytic mechanism of aspartate aminotransferase"
Dr. E.L. Mehler, Biozentrum, Univ. Basel

"Combining protein molecular dynamics with 3-D profiles and atomic solvation parameters"
Dr. R. Luethy, ISREC Lausanne

Chemistry

"Ab-initio Berechnung zwischenmolekularer Wechselwirkungen und deren Verwendung in Simulationen von Flüssigkeiten"
Prof. H. Huber, Inst. für Physikalische Chemie, Univ. Basel

"Quantum chemical computation of large molecules"
Dr. H.P. Lüthi, IPS, ETHZ

"Monte Carlo Simulationen von Polymeren"
Prof. U. Suter, Inst. für Polymere, ETHZ

"Quantum chemical investigation of organometallic complexes" "Modelisation de la structure et des proprietes catalytiques de zeolithes" "Etudes des reconstructions de surface et de l'adsorption d'hydrogene dans les semiconducteurs"
Prof. J. Weber, Dep. de chimie physique, Univ. Genève

"Spectroscopy and dynamics of molecules and clusters"
Prof. M. Quack, Lab. für Physikalische Chemie, ETHZ

Engineering

"Computation of unsteady three-dimensional flows in complex geometries"
Prof. M.K. Eberle, Inst. für Energietechnik, ETHZ

"Device- und Prozess-Simulation"
Prof. W. Fichtner, Inst. für Integrierte Systeme, ETHZ

"Motion analysis and recognition in image sequences" "Digital image sequence processing and coding"
Prof. M. Kunt, Lab. de traitement des signaux, EPFL

"Teilchenwachstum in laminarer und turbulenter Flüssigkeitsströmung"
Prof. F. Rys, Dr. W. Miller, Lab. für Technische Chemie, ETHZ

"Subsonische Strörmungen um stumpfe Körper"
Prof. B. Müller, Inst. für Fluiddynamik, ETHZ

Environmental Sciences

"High resolution climate simulations" "Simulations of the influence of the Alps on climate" "Simulations of the ozone layer depletion"
Dr. M. Beniston, Geographisches Inst., ETHZ

"Development of a ray tracing model to simulate the transfer of radiation in arbitrary complex systems"
Dr. M. Verstraete, IRSA, JRC Ispra (I)

Physics

"Quantum simulation of materials"
Prof. R. Car, IRRMA, EPFL

"The continuum limit of SU(2) lattice gauge theory"
Dr. K. Decker, Inst. für Informatik und Angewandte Mathematik, Univ. Bern

"Critical dynamics, Lanczos algorithm"
Dr. M. Henkel, Dép. de physique théorique, Univ. Genève

"Elastic and dynamical properties of solids" "Heavy fermions" "Study of high Tc compounds" "Electronic structure of disordered materials"
Dr. T. Jarlborg, Dép. de physique de la matière condensée, Univ. Genève

"Monte Carlo simulation of weak hadronic matrix elements in quantum chromodynamics on the lattice"
Dr. F. Jegerlehner, PSI

"Numerical simulation of cluster deposition on surfaces"
Dr. C. Massobrio, Inst. de physique expérimentale, EPFL

Berechnung der elektronischen Struktur von Störstellen in Festkörpern"
Prof. P.F. Meier, Physik-Inst., Univ. Zürich

"Density functional molecular dynamics"
Dr. I. Moullet, Section de physique, Univ. Lausanne

"Zusammenstossende Sternwinde in Symbiotischen Doppelsternsystemen"
Prof. H. Nussbaumer, Inst. für Astronomie, ETHZ

"High-temperature expansions"
Prof. T.M. Rice, Dr. W. Putikka, Inst. für theoretische Physik, ETHZ

"Ab-initio simulation of a biomaterial: the clean and hydroxilized TiO2 surface"
Prof. S. Steinemann, Inst. de physique expérimentale, Univ. Lausanne

"Wachstumsmodelle und ihre Beschreibung durch Kontinuumsgleichungen"
Dr. G. Zumofen, Lab. für Physikalische Chemie, ETHZ

"2D linear/cubic finite elements code to solve linear wave equations of a warm plasma"
Dr. K. Appert, CRPP, EPFL

"CE-Alloys: electronic and magnetic properties of CE compounds"
Prof. P. Erdoes, Univ. Lausanne
Dr. P. Monachesi, Univ. L'Aquila (I)

"Numerische Verfahren zur Simulation stark wechselwirkender fermionischer Systeme"
Dr. D. Würtz, IPS, ETHZ

Physics

MHD Equilibrium and Stability Codes for Tokamak Plasma with Separatrix

S. Medvedev [a, b], R. Gruber [c, d], G. Jost [e] and S. Merazzi [c]

[a]Centre de Recherches en Physique des Plasmas
Association Euratom - Confédération Suisse
Ecole Polytechnique Fédérale de Lausanne
Lausanne, Switzerland

[b]Keldysh Institute of Applied Mathematics
Moscow, Russia

[c]Centro Svizzero di Calcolo Scientifico
Manno, Switzerland

[d] Service Informatique Central
Ecole Polytechnique Fédérale de Lausanne
Lausanne, Switzerland

[e] NEC Germany

Introduction

Magnetohydrodynamic (MHD) equilibrium and stability codes were extensively used for tokamak plasma studies during the last 15 years. Most of the results were obtained for conventional plasma equilibrium configurations with nested magnetic flux surfaces inside the plasma [1]. Much less efforts were made to investigate the case of a plasma with a separatrix, the magnetic surface going through an x-point where the poloidal magnetic field vanishes [2]. On the other hand, a plasma with an external separatrix is the configuration used in modern tokamaks to obtain better confinement. The doublet configuration with an internal separatrix has a number of possible advantages and can be of interest in experiments with a highly elongated cross-section plasma as the one of the TCV tokamak at EPFL.

New codes make it possible to extend equilibrium and stability studies to a wider range of tokamak plasma configurations with separatrix. The paper describes the models used and the code implementation on the NEC SX-3 computer.

Equilibrium

An axisymmetric plasma equilibrium is described by the Grad-Shafranov equation

$$\nabla \cdot \left(\frac{\nabla \psi}{r^2}\right) = -\frac{j_\varphi}{r} \qquad j_\varphi = r\frac{dp}{d\psi} + \frac{1}{r}F\frac{dF}{d\psi}$$

where $\psi(r, z)$ - poloidal flux function, p - plasma pressure, j_{φ} -toroidal current density. The magnetic field can be represented as $\boldsymbol{B} = \nabla\psi \times \nabla\varphi + F(\psi)\nabla\varphi$, (r, z, φ) - polar coordinates.

The domain is decomposed into subdomains inside and outside the separatrix. Picard iterations on the nonlinearity in the right hand side term are combined with mesh adaptation to magnetic surfaces which are nested in each subdomain (Figure 1). Mesh adaptation instead of mapping provides very accurate coordinates of $\psi = const$ surfaces used as input for the stability code. The inversion of the elliptic operator is numerically performed with an iterative matrix solver using a highly vectorizable 4-color Gauss-Seidel method with overrelaxation. The solver allows to take full advantage of domain decomposition [3]: matrices for each subdomain can be assembled and stored separately. Connectivity conditions between subdomains can be applied to diagonal matrix elements and resulting vectors only. Periodicity conditions can be treated in the same way.

The most computationally intensive part of the code is the iterative matrix solver. The main operations here are essentially multiplications of 9-band matrices with vectors which are vectorized by the f77sx FORTRAN compiler: the resulting speed is 370 Mflops at a vector length close to the maximum of 128. For some operations in the 4-color solver, the vector length is shorter. For the typical case of an up-down symmetric equilibrium with dimensions of 64*64 for the domain inside the separatrix and of 32*64 for the outside, the run takes 20s CPU time at 240Mflops and an averaged vector length of 55.

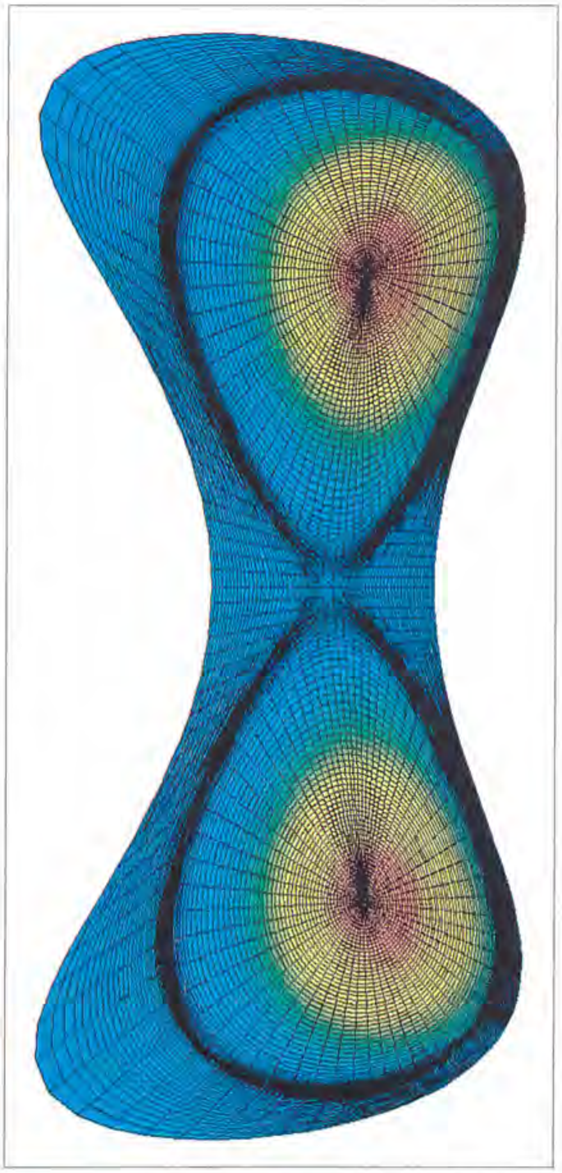

Figure 1: Mesh adapted to magnetic surfaces and tooroidal current density for up-down symmetric equilibrium with internal separatrix.

Stability

The linearized ideal MHD eigenvalue equations for a plasma displacement $\xi e^{i\omega t}$ around equilibrium can be written in their variational form [4]:

$$\delta(W(\xi, \xi) - \omega^2 K(\xi, \xi)) = 0$$

The quadratic functionals $W(\xi, \xi)$ and $\omega^2 K(\xi, \xi)$ correspond to the potential and kinetic energy of the plasma displacement, respectively. A negative eigenvalue ω^2 corresponds to an unstable growing in time solution.

For axisymmetric equilibria, $\xi_n e^{in\varphi}$ modes with different toroidal wave numbers n are decoupled and the problem becomes two-dimensional for each ξ_n. Using a so-called flux coordinate system (ψ, θ, φ), one can see that no derivatives with respect to ψ of tangential to magnetic surfaces components of ξ enter the variational form. This fact leads to noncompactness of the operator corresponding to an eigenvalue spectrum with continuous parts and cluster points [5]. To represent correctly the physics, flux coordinates and hybrid finite elements [6] are used. Some further peculiarities in choice of approximation were employed to improve convergence of the code: spectral shift elimination [7] and numerical destabilization correction [8]. A vacuum layer between the plasma region and the external perfectly conducting wall can be included into the model using the "pseudodisplacement" approach [9].

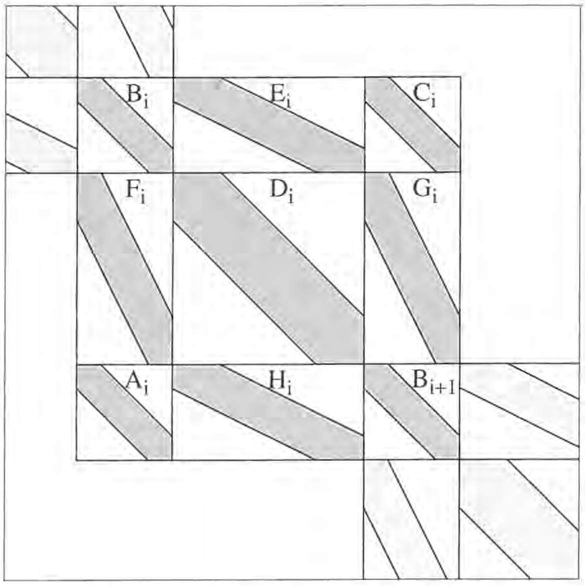

Figure 2. Matrix structure for stability problem.

A direct matrix decomposition method combined with an inverse vector iteration are used for solving the corresponding matrix eigenvalue problem. The structure of the matrix for each subdomain is shown in Figure 2. The solver is based on the PAMERA solver [3]. Nonoverlapping parts of the blocks can be eliminated in parallel for all blocks in each subdomain. The resulting matrix structures for the ξ^{ψ} component are block three-diagonal which can be eliminated separately for each subdomain, the ones at the separatrix remain. The final connectivity assembling consists of overlapping these remaining blocks.

In the first version of the solver, the band structure of the matrix blocks was not taken into account. Full matrix inversion, matrix*matrix and matrix*vector operations were performed with highly optimized routines. The overall code performance for a 3 subdomain case with dimensions of 64*64 + 64* 64 +16*128 reaches 1.5Gflops (20s CPU time). Memory size is already 800Mb in this case. In the second version of the solver, the subblocks D, E, F, G, H (Figure 2) are stored as band matrices. Specially written FORTRAN routines are used for a band matrix*vector operation, an LU band matrix decomposition, a band $(LU)^{-1}$*vector and a $(LU)^{-1}$*matrix operations. For the above mentioned 3-subdomain case we have 500Mflops and 10s CPU time against 20s with a full block solver. The memory requirement measured also diminishes, leading to a doubling of the treatable case: 920Mb for 128*128 + 128*128 + 32*256. For these dimensions the performance reaches 900Mflops due an to increased relative time for full matrix operations (70s CPU time).

Results

The developed codes have been validated with various convergence studies and benchmarking with other codes. Up-down symmetric equilibria with an internal separatrix were computed. Stability criteria for high-n ballooning and localized Mercier modes were implemented and applied to the equilibria. In Figure 1, the mesh adapted to magnetic surfaces and the toroidal current density distribution are shown for an equilibrium configuration with vacuum outside the separatrix. For this case, the pressure profile was optimized against localized ballooning mode stability. For this type of equilibria limiting values of β (the ratio between the gasokinetic and magnetic pressures inside the plasma) were computed against the external $n = 1$ kink instability. There are two branches of the instability corresponding to two different solutions outside the separatrix. The level lines of the displacement component normal to magnetic surfaces are shown in Figure 3 for the most unstable eigenmode. The β -limits are found to be in correspondence with known scalings for conventional tokamaks.

The codes run fast on the SX-3 machine. For example, the stability code applied to a one plasma domain case is about 5 times faster than the analogous code ERATOA on CRAY-2 [2]. High performance is reached using optimized routines for matrix operations. Enhancement of the performance is possible with further band matrix routines optimization.

References

[1] Troyon, F., R. Gruber, H. Sauren, S. Semenzato and S. Succi. *Plasma Phys.* 26 (1984): 209.

[2] Roy, A. EPF Lausanne Thesis (1990).

[3] Gruber, R., W. A. Cooper, M. Beniston, M. Gengler, and S. Merazzi. *Phys. Reports* 207(1991): 167.

[4] Bernstein, I. B., E.A. Frieman, M.D. Kruskal and R. M. Kulrud. *Proc. Roy. Soc.* A244 (1958): 17.

[5] Rappaz, J. *Numerical Mathem.* 28 (1977): 15.

[6] Gruber, R. *J. of Comput. Phys.* 26 (1978): 379.

[7] Gruber, R. and J. Rappaz. "Finite Element Methods in Ideal Linear Magnetohydrodynamics." (Springer series in computational physics, Springer, 1985).

[8] Degtyarev, L. M. and S. Yu. Medvedev. *Computer Phys. Commun.* 43 (1986): 29.

[9] Gruber, R., S. Semenzato, F. Troyon, T. Tsunematsu, W. Kerner, P. Merkel and W. Schneider. *Computer Phys. Commun.* 24 (1981): 363.

Figure 3: Level lines of normal to magnetic surfaces component of plasma displacement. Most unstable external n=1 kink mode.

Calculation of X-ray Absorption Spectra: Comparison with Experiment and Predictions

P. Lerch and T. Jarlborg
DPMC
Université de Genève
Genève, Switzerland

Abstract

Local density calculations for $CoSi_2$ and for the strongly enhanced paramagnet ZrV_2 have been performed. The extraction of a core electron may produce a local spin polarization near the nucleus, which sometimes induces magnetism among valence electrons depending on the core hole. Two supercell calculations are presented; one in which the screening of the core hole has no spin-dependence and one where it is strongly spin-dependent.

Introduction

In X-ray absorption measurements, a core electron is excited above the Fermi level, making the absorption a symmetry and site dependent probe of the unoccupied density-of-states (DOS). According to the final state rule (FSR), the X-ray absorption spectra should be calculated in the final state, i.e. in the presence of the core hole [1]. It has been verified that calculated valence states which have been modified by the core hole, agree better with experiment than the ground state bands [2]. This does not concern systems with filled bands in which correlation may be strong [3]. In general, the FSR has been applied in the non spin-polarized case, but in some cases the scattering may be strongly spin dependent [4]. The screening potential should be spin dependent in order to satisfy the Friedel sum rule for the phase shifts. This strong spin-dependence has been seen for the case of Li [4]. Experimental evidence of the importance of exchange effects has also been found for the case of other alkali metals [4].

Here we will present calculations for two materials. The first is a calculation of the L_3-edge X-ray absorption spectrum (XAS) of $CoSi_2$, a metallic non-magnetic compound. The second concerns K, L_3, and M_3-edges of V for the Stoner enhanced ZrV_2, where the core hole induces locally a magnetization among valence states. Here we concentrate on the L_3-edges, since the L_3 XAS is a probe of the *d*-density-of-states (DOS). Due to their localization, *d*-electrons are much more affected by a core-hole than *s* or *p*-electrons. Thus these screening effects are seen more clearly in the *d*-DOS.

Screening in $CoSi_2$.

We performed all electronic structure calculations with the self-consistent linear muffin-tin (LMTO) method [5] in the local density approximation (LDA). The structure of $CoSi_2$ is of fluorite type. The elementary cell contains one Co atom and two Si atoms. We added an empty sphere in order to obtain a good space filling. Our basis set includes *s*, *p* and *d*-orbitals.

To compute the L_3-edge of Co, we have to perform the electronic structure calculation with a $2P_{3/2}$ core hole on a Co site, according to the FSR. This means doing a supercell calculation in order to allow the excited system to relax. For $CoSi_2$ we used a four times bigger cell. The initial cell is FCC and the supercell is SC. This satisfies the thumb rule that one should take two shells of unperturbed atoms around each ionized atom. In many cases a single shell is sufficient for the threshold energies while details of the spectra may change when going from one to two shells. The difference between doing the calculations with and without a supercell is shown in Figure 1. The $CoSi_2$ compound is non-magnetic in the ground state and remains non-magnetic in the excited state.

Whereas for the Si K-edges, predictions from the FSR have been verified [2], the question is much more difficult for the Co L_3-edge. We show in Figure 2 the L_3-edge spectra for Co such as it should be experimentally observed (matrix elements and broadening are included). Here one sees the importance of doing supercell calculations. The supercell FSR spectra is very similar to the initial state. A different conclusion would be drawn without a supercell [2]. Thus the question whether the FSR applies to Co L_3-edges, can not be decided in this particular case. Here the one-electron picture has also to be questioned because of the correlation in the nearly filled *d*-bands of Co. Despite these doubts, it turns out that threshold energies agree well with experiment when the FSR is followed [2].

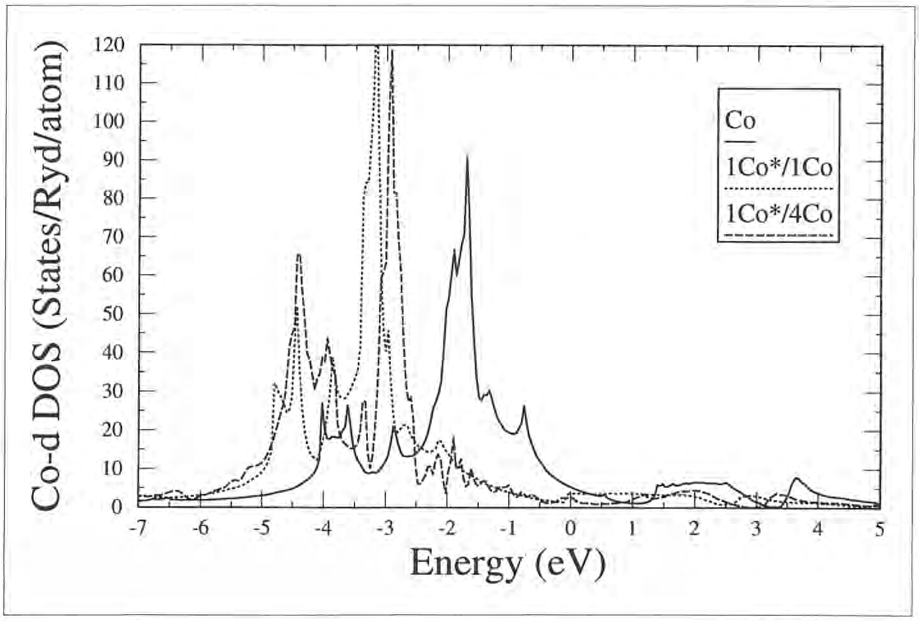

Figure 1: Co *d*-DOS for $CoSi_2$. We show the *d*-DOS for the ground state (continuous) and for two FSR calculations: for an elementary cell (dotted) and for a supercell calculation (dashed). The energy is relative to E_F.

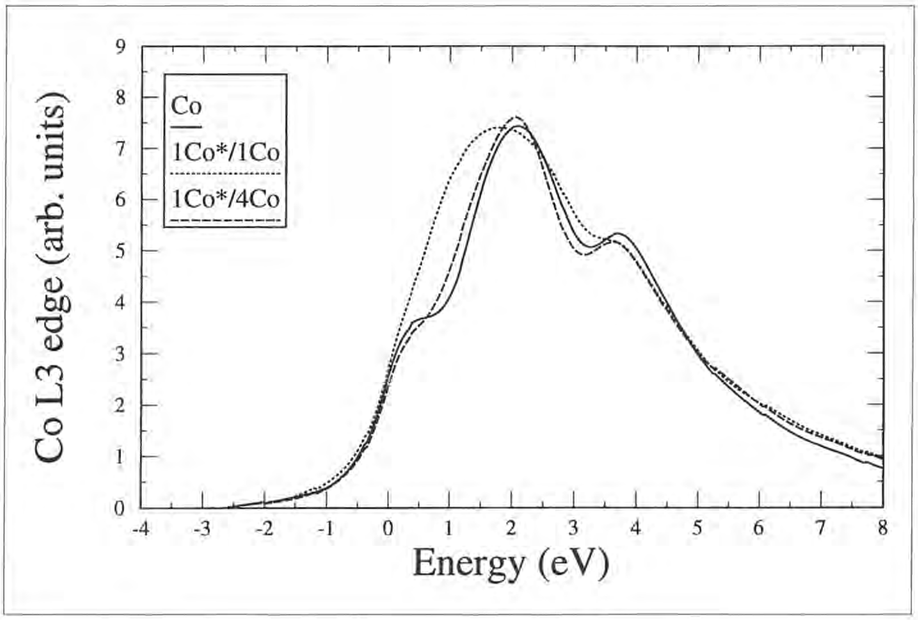

Figure 2: XAS L_3-edge of Co in $CoSi_2$ (including core hole effects and matrix elements) for the final state as obtained from an elementary cell (dotted) and from a supercell (dashed) calculations. The initial state calculation (continuous) is close to the supercell FSR spectra. A Lorentzian broadening due to the lifetime of the corehole and the excited band-states plus a Gaussian broadening simulating experimental resolution have been included. The energy is relative to E_F.

Spin-dependent Screening in ZrV_2.

Strongly enhanced paramagnets, like ZrV_2, are interesting test cases for the FSR, since the ground-state is non spin-polarized (non-SP), while the final state for the absorption process becomes spin-polarized by the core hole. The important effect here is that the exchange interaction between remaining electrons in a partially filled core orbital and the valence electrons is strong enough to induce magnetization if the overlap between the ionized core orbital and the valence states is sufficient. If this is the case, the valence states are polarized by the core hole, and the system relaxes to a lower total energy than if no spin polarization is allowed. The magnetism is induced locally at and near the site with a core hole, and has not the same properties as a spontaneous, itinerant spin fluctuation. Here we discuss this effect in ZrV_2.

The ground state of ZrV_2 in the C15 structure is non-magnetic but close to a magnetic transition [6]. The elementary cell contains 2 Zr and 4 V atoms. The LMTO supercell calculations contained a *s*, *p*, *d* basis. The supercell is four times the elementary cell, i.e. 1 out of 24 atoms is ionized. [7].

Our total energy calculations show, that at the experimental lattice constant a=7.445Å, the ground state is non-magnetic but only 1 mRyd lower than the spin-polarized (SP) state. However, SP and non-SP total energy calculations with different coreholes (1S, 2S, $2P_{1/2}$, $2P_{3/2}$, 3S, $3P_{1/2}$, $3P_{3/2}$), show that the FM states are favoured. For all the core holes considered, the SP results are systematically lower than the non-SP by several eV (Table 1). From the total energies we get also accurate values for the threshold values. These values are obtained as the total energy difference between the non-perturbed state and the relaxed cell calculation, which correspond to the so-called ΔSCF values. Threshold values for the SP and non-SP cases are also shown in Table 1. Here we neglect dynamical effects which would be accounted for in the GW approximation. On the other hand, the ΔSCF method contains highly non-linear terms which are known to be more important, especially for shallow orbitals, or for doubly ionized core-orbitals.

In the last column of Table 1 we show the induced moments for the different core holes. We see that mainly the V *d*-electrons are polarized while the *s* and *p*-electrons are only slightly affected. The reason is that the more localized *d*-electrons are very affected by the more attractive potential in the presence of the corehole. It is seen that the polarization of the V* *d*-electrons is negligibly small for the quantum number n=1, while they are of order 1.8 μB for n=2 and 2.3 μB for n=3. This tendency can be understood from the fact that the overlap with band-states is very small for the 1*S* core orbital and increases strongly for outer core orbitals.

Of special interest is the L_3-edge. As the transition probability is roughly 50 times more probable from 2P core states to *d*-band-states than to *s*-band-states, the L_3-edge reflects essentially the V-*d* DOS which is strongly affected by the corehole.

Figure 3 shows SP and non-SP spectra with core hole effects included. For the $L_{2\text{-}3}$-edge, the spin-orbit coupling is calculated to be 7.1 eV, which means that L_2 and L_3 spectra can be seen separately. The core hole lifetime broadening is 0.25 eV and the difference between SP and non-SP XAS is resolved even after the broadening. This is a prediction from FSR and LDA. It also predicts that the so-called circular magnetic X-ray dichroism (CMXD) [8] reflecting the spin dependent DOS, should be strongly reflected by the magnetic final state. However, two-hole spectra are calculated to be non-magnetic.

Conclusions

The validity of the FSR has been verified for Si K-edges in several disilicides. For the Co L_3-edge in $CoSi_2$, both FSR and initial state rule lead to the same spectra after a realistic broadening.

Table 1: Threshold values obtained by SP and non-SP calculations (in eV) are reported in the first two columns. The third column shows the difference between non-SP and SP threshold energies (in eV), which is equal to the difference in total energies. Last column shows the induced moments for *d*-electrons on the ionized V site. The induced moments on adjacent sites are always very small.

Edges	Holes	non-SP	SP	$\Delta E_{nSP\text{-}SP}$	V*-d (μM)
K_1	1S	5471	5447	23.7	-0.1
L_1	2S	607.8	605.8	2.0	1.6
L_2	$2P_{1/2}$	518.4	517.0	1.4	1.8
L_3	$2P_{3/2}$	511.0	509.1	1.9	1.8
M_1	3S	63.4	61.9	1.5	2.2
M_2	$3P_{1/2}$	38.0	37.0	1.0	2.3
M_3	$3P_{3/2}$	37.2	36.2	1.0	2.3

For Stoner enhanced paramagnets, like ZrV_2, the FSR predicts spectra from a locally magnetic final state. The induced magnetic moments are essentially *d*-like. They depend on the strength of the overlap between the ionized core orbital and the band-states. The results predict a clear signature of the magnetic state in form of unusual L_3 XAS and modified threshold energies. Therefore, X-ray measurements in ZrV_2 provide an interesting test case of the FSR in a system with strong spin dependent screening.

List of Publications

[1] Nozières, P. and C. T. De Dominicis. 178 (1969): 1097.

[2] Lerch, P., T. Jarlborg, V. Codazzi, G. Loupias and A. M. Flanck. *Phys. Rev. B* 45 (1992): 11481.

[3] Zaanen, J., M. Alouani and O. Jepsen. *Phys. Rev. B* 40 (1989): 837.

[4] Almbladh, C. O. and L. Hedin. In *Handbook on Synchrotron Radiation*, edited by E.-E. Koch. Amsterdam: North-Holland (1983) Vol. 1b, p. 607.

[5] Andersen, O. K. *Phys. Rev. B* 12 (1975): 3060; T. Jarlborg and G. Arbman, *Journal Physics* F 7 (1977): 1635.

[6] Jarlborg, T. and A. J. Freeman. *Phys. Rev. B* 22 (1980): 2332; B. M. Klein, W. E. Pickett, D. A. Papaconstantopoulos and L. L. Boyer. *Phys. Rev. B* 27 (1983): 6721; M.-C. Huang, H. J. F. Jansen and A. J. Freeman. *Phys. Rev. B* 37 (1988): 3489

[7] Lerch, P., E. G. Moroni and T. Jarlborg. (to be published).

[8] Schütz, G., R. Wienke, W. Wilhelm, W. Wagner, P. Kienle, R. Zeller, and R. Frahm. *Z. Phys. B* 75 (1989): 495.

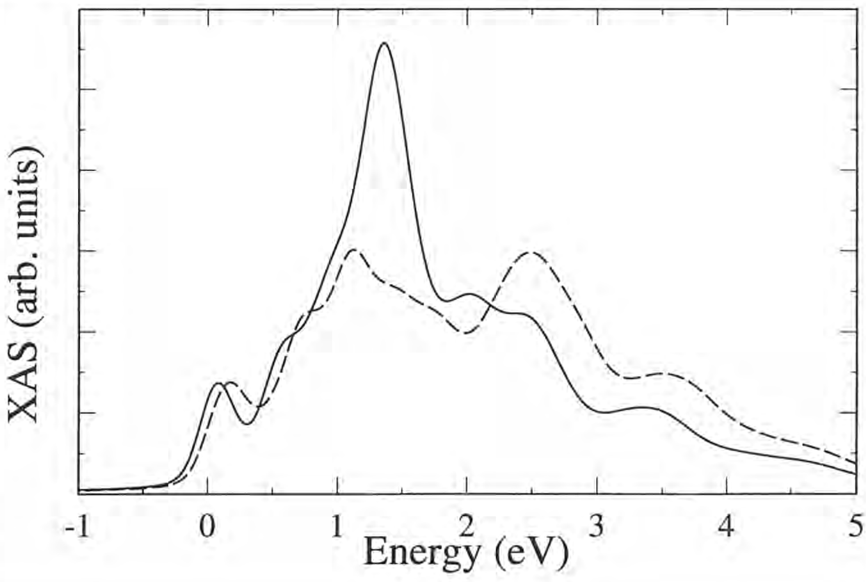

Figure 3: XAS L_3-edge of V in ZrV_2 (including core hole effects and matrix elements) for the SP final state (dashed) and the non-SP (continuous) calculation. A Lorentzian broadening due to the lifetime of the core-hole (0.24 eV) and the excited band-states (0.05*|E-E_F|), plus a Gaussian broadening simulating experimental resolution (0.1 eV) have been included in order to approach realistic experimental spectra. The energy is relative to E_F.

Monte Carlo Simulation of Weak Hadronic Matrix Elements in Quantum Chromodynamics on the Lattice

C. Alexandrou [a], S. Güsken [b], F. Jegerlehner [a],
K. Schilling [b] and R. Sommer [c]

[a]Paul Scherrer Institut
Villigen PSI, Switzerland
[b]Physics Department
University of Wuppertal
Wuppertal, Germany
[c]Theory Division, CERN
Geneva, Switzerland

In this project we calculate simple properties of B-mesons, bound-states of a heavy antiquark ($\bar{b}$) and a light quark (u, d or s). The B-meson system provides a new challenge for lattice calculations since all other attempts to predict properties of B-mesons from first principles have failed so far. The main goal is to predict the decay constant f_B. f_B is the key parameter for the B-meson system and as yet could not be determined experimentally. Its value crucially affects the observability of the still mysterious phenomenon of violation of time-reversal symmetry in elementary particle processes.

Quantumchromodynamics (QCD) is the fundamental theory of strong interactions which describes subnuclear phenomena like the interaction between protons and neutrons in atomic nuclei. QCD predicts that all strongly interacting particles (hadrons) are made up of triplets of quarks and antiquarks which are permanently confined inside hadrons by an octet of gluons. The binding energy may exceed the mass of the constituents by more than one order of magnitude. Therefore perturbative methods completely fail for describing strongly interacting bound states.

QCD on the lattice is a non-perturbative approach to the strong interaction dynamics. The infinite space-time continuum is approximated by a finite L^3 x T lattice with finite lattice spacing a. L is the number of points in a spatial direction and T is the number of points in the time direction. This approach provides the only known method to calculate i) masses and wavefunctions of baryons and mesons, ii) transition matrix-elements between hadronic states, iii) phase transitions to new forms of matter like the quark-gluon plasma and other strong coupling problems.

In lattice QCD to each point x of a space-time lattice a quark field ψ_x is attached. This field is represented by 3(color) x 4(spin) complex numbers. To each link connecting two neighboring points x and y a gluon field $U(x, y)$ is attached. It is represented by an element from , the group of unitary 3 x 3 matrices with determinant unity. The dynamics is determined by the action

$$S(U, \psi, \bar{\psi}) = -\frac{\beta}{6}\sum_{P} Tr\,(U_P + U_P{}^{\dagger}) + \sum_{x,y} \bar{\psi}_x M_{x,y} \psi_y$$

Here, U_P is a product of 4U's around an elementary square p, and $M_{x,y}$ is the complex N x N fermion matrix, where $N = 12 \times L^3 \times T$. For L=18 and T=48 the fermion matrix has $2N \cong 6.7 \times 10^6$ real entries, for example. An observable is determined by a statistical average with weight factor e^{-S}

$$\langle O \rangle = \int \prod_{lattice} dUd\bar{\psi}d\gamma\psi O\,(U, \psi, \bar{\psi})\, e^{-S\,(U,\,\psi,\,\bar{\psi})}$$

This is a $D = 80 \times T^3 \times T$ dimensional integral. For the lattice size in the previous example we have $D \cong 22.4 \times 10^6$. Such integrals can be evaluated by the Monte Carlo integration method. One generates random configurations $\{U\,(x, y)_i, \psi_{xi}, \bar{\psi}_{xi}\}$ which are distributed according to the weight e^{-S} and calculates

$$\langle O \rangle \approx \frac{1}{N} \sum_{i=1}^{N} O\,(U, \psi, \bar{\psi})$$

for $N \rightarrow \infty$. Present computational capabilities make necessary further approximations. First, one generates the configurations $\{U\,(x, y)_i\}$ (using Metropolis updating) independently of the quark fields. Second, since the action is bilinear in the quark fields the latter can be integrated out analytically. This yields expressions in terms of the quark propagators $\langle \psi_{x'}, \bar{\psi}_x \rangle = \Delta_{x',\,x}$ which are obtained by solving $\sum_{x'} M_{x,\,x'} \Delta_{x',\,y} = \delta_{x,\,y}$ by the conjugate gradient method for inversion of huge sparse matrices. The fermion determinant $det\,(\Delta_{xy})$, which is obtained by the integration, is approximated by unity.

The B-meson decay constant and mass are obtained by analyzing the correlation function of the time component of the axial-vector current

$$C\,(t) = \sum_{\vec{x}} \langle A_o\,(\vec{x}, t)\, A_0^{\dagger}\,(0, 0) \rangle \underset{t \rightarrow \infty}{\rightarrow} \frac{f_B^2 M_B}{2} e^{-M_B t}$$

Preliminary results were obtained on CRAY's [1]. Using the NEC SX-3[1] we were able, for the first time, to perform a high statics calculation which allows for a much better control of the systematic errors. From the data obtained for the lattices listed in Table 1 we can now study more extensively

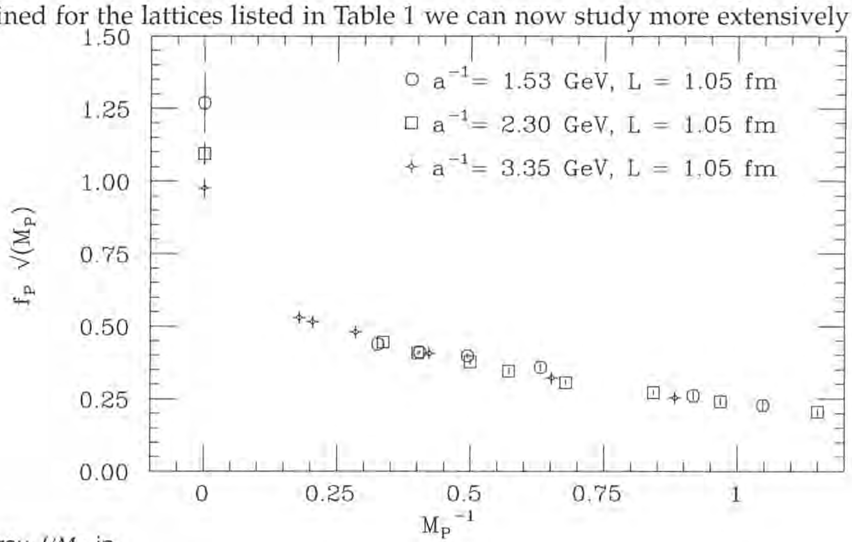

Figure 1. $f_P\sqrt{M_P}$ in $GeV^{3/2}$ versu $1/M_P$ in GeV^{-1} at β = 5.74, 6.0 and 6.26. The results at $1/M_P$=0 are obtained in the static limit. f_B is the value of f_p at M_P=M_B ≈ 5 GeV.

---

[1] Our code runs with an overall performance of 660 Mflops (31% of the time is spent in two subroutines which exhibit a performance of about 90 Mflops). This is about four times the performance obtained on a Cray Y-MP. The performance is mainly by memory access [2].

b	L/a	L_t/a	N	a^{-1}/geV	L/fm
5.74	4	24	404	1.45(19) [1.12]	0.55
	6	24	131		0.82
	8	24	270		1.10
	10	24	213		1.37
	12	24	140		1.65
5.82	6	28	100	1.72	0.70
6.00	6	36	227	2.25(10) [1.88]	0.53
	8	36	100		0.70
	12	36	304		1.05
	18	36	27		1.58
6.26	12	48	103	3.70(32) [2.88]	0.64
	18	48	76		0.96

Table 1: Lattices used in this work. N gives the number of independent configurations. The inverse lattice spacing a^{-1} in GeV is normalized by the ρ meson mass. The spatial extension *L* is given in fermi (fm).

finite a and volume effects as well as go to smaller quark masses. We have already analysed our results for the static approximation [3] and we are at present analysing the results for finite m_h (see Figure 1).

From this study we found

$$190 \le f_B \le 240 MeV$$

The error above arises from various sources: i) statics which means one needs larger *N*, ii) $a \rightarrow 0$ extrapolation, iii) extrapolation to the u-quark mass limit (or chiral limit).

The last error arises because as we decreased the quark-mass the fermion matrix *M* has a singular behaviour, it behaves like $1/m_{\text{quark}}$ and therefore the time required to find the inverse grows. On the CRAY for the largest lattice we were unable to reach small enough masses.

The analysis of the results obtained in the static approximation settles a number of issues which were up to now unclear.

List of Publications

[1] Alexandrou, C., S. Güsken, F. Jegerlehner, K. Schilling andR. Sommer. *Physics Letters* B256 (1991): 60; *Nuclear Physics B* 374 (1992): 263; R. Sommer, C. Alexandrou, S. G F. Jegerlehner, K. Schilling. *Nuclear Physics B* (Proceedings Supplement) 20 (1991): 493; *Nuclear Physics B* (Proceedings Supplement) 26 (1992) 387; C. Alexandrou. *Speedup Journal* 6(1) (1992): 41.

[2] Barker, D.P. . CSCS Manno, private communication.

[3] Alexandrou, C., S. Güsken, F. Jegerlehner, K. Schilling and R. Sommer. PSI-PR-92-27; PSI-PR-28, to appear in " Lattice '92" *Nuclear Physics* (Proceedings Supplement). C. Alexandrou and F. Jegerlehner. Crosscuts (CSCS newsletter) Vol.1(3) (1992): 10.

Calculation of Molecular Properties in Liquids and Bulk Properties of Liquids

R. Eggenberger, S. Gerber, H.P. Huber, D. Searles and M. Welker

Institut für Physikalische Chemie
Universität Basel
Basel, Switzerland

Theoretical predictions of properties of small and medium sized single molecules have reached a quality comparable to experiment. These predictions are quite valuable in connection with gas phase experiments, e.g. several kinds of spectroscopy. However, the bulk of chemistry does not deal with single molecules but with reactions of molecules and with the liquid phase. This work is heading towards progress in the prediction of the liquid phase properties mainly from pure theory without using any empirical data. We have chosen two different approaches, one heading towards the prediction of bulk properties of liquids and one towards the prediction of local properties in molecules in liquids.

For the first approach we selected liquid neon as a very simple system. The potential curve of the neon dimer was obtained from quantum chemical ab initio calculations and then applied in classical equilibrium molecular dynamics (MD) simulations to obtain many properties of neon in the liquid and supercritical state. Most properties, like the second virial coefficient, the shear viscosity, the thermal conductivity, the diffusion coefficient, the state function, the molar heat capacity, the internal energy and the enthalpy and the pair correlation function were obtained with typical accuracies between 5 and 15%, which is a fair result for a purely theoretical prediction. However, more important is the fact that we have produced benchmark results which will now allow investigation of which approximations were the most poor, and then improvements of the results.

For the second approach we decided to calculate the deuterium quadrupole coupling constant (DQCC) of liquid heavy water. Previously, we had calulated DQCC's for many molecules in the gas phase and reached an accuracy of about 3%. For the liquid we developed and tested a new approach. Taking a dimer potential from the literature obtained with quantum chemical ab initio calculations, we performed equilibrium MD simulations at a given temperature and took snapshots of the molecular coordinates. To calculate the DQCC for a certain deuterium, a water cluster of 5 molecules with the deuterium of interest in the center, as shown in the figure, was taken from a snapshot and used for a quantum chemical ab initio calculation in a supermolecule ansatz. This was repeated for roughly 100 snapshots to obtain a statistical average. Repeating the whole procedure at different temperatures and pressures yielded the temperature- and pressure-dependence of the DQCC. The results are encouraging being within the experimental errors.

The simulation program used for neon was written in standard FORTRAN77 and runs on many computers. It was used for a comparison (see first reference below) of performance on many different machines. For the vector-processors a slightly different algorithm was used yielding a speed about 120 times that of a VAX-8800 processor.

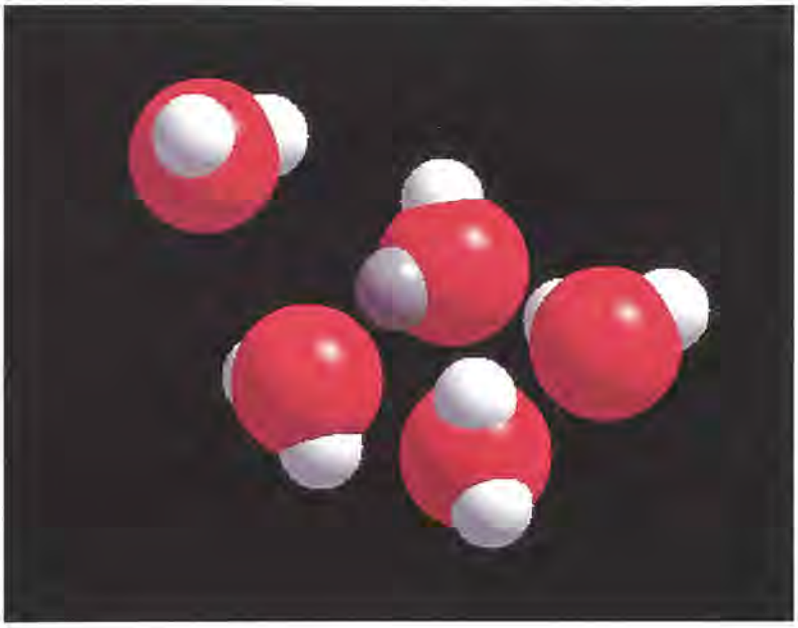

List of Publications

[1] Eggenberger, R. and H. Huber. "Comparison of the Performance of a Program for Molecular Dynamics of Liquids on Different Computers." *CHIMIA* 46 (1992): 227.

[2] Eggenberger, R., S. Gerber, H. Huber, D. Searles and M. Welker. "*Ab initio* Calculation of the Shear Viscosity of Neon in the Liquid and Hypercritical State Over a Wide Pressure and Temperature Range." *Chem. Phys.* 164 (1992): 321.

[3] Eggenberger, R., S. Gerber, H. Huber, D. Searles and M. Welker. "*Ab initio* Calculation of the Thermal Conductivity of Neon in the Liquid and Hypercritical State Over a Wide Pressure Range." *Molec. Phys.* 76 (1992): 1213.

[4] Eggenberger, R., S. Gerber, H. Huber, D. Searles and M. Welker. "*Ab initio* Calculation of the Deuterium Quadrupole Coupling in Liquid Water." *J. of Chem. Phys.* 97 (1992): 5898.

Computational Chemistry 1992

J. Weber

Department of Physical Chemistry
University of Geneva
Geneva, Switzerland

It is now beyond argument that computational chemistry (CC) has recently evolved from the stage of an esoteric tool employed by highly specialized scientists into a mature discipline with important applications used by chemists in their daily work. Suffices here to recall the spectacular enhancements in chemical instrumentation or the tremendous progress in molecular modelling, limiting ourselves to these two examples, brought about by computers.

It is indeed no overstatement to assert that CC belongs today to the family of indispensable tools in chemistry, as much as NMR or X-ray crystallography. However, the main difference with these tools is that computerized applications offer an incredibly large spectrum in chemistry, ranging from the integration of chemical formulae within text processing on a PC to the simulation of new materials on a supercomputer.

It is therefore necessary to select our topic in this short presentation and, leaving aside some subfields of CC such as chemometrics, structure elucidation, the processing of chemical information, structural data bases, etc. we shall concentrate on *molecular modelling* and *computational quantum chemistry*.

Molecular modelling may be defined as the construction and utilization of models (i.e., simplified representations) to rationalize and predict molecular structures, properties and interactions. Contrary to a generally received opinion, molecular modelling does not necessarily involve graphics as the computerized models may consist of numbers only. However, in view of the progresses recently achieved in what is known today as scientific visualization, molecular modelling would be generally of little value to the community of chemists without the use of computer graphics, which leads naturally to molecular graphics (MG). MG has become an important tool in computer-assisted chemistry: as evidenced by the various applications performed today, the role of MG consists not only in visualizing molecular structures and properties, but also in interacting with simulations in real time, changing the building blocks of the investigated compounds, comparing geometries, displaying scenarios in which substrates dock and bind to macromolecules, etc. Without exaggeration, it is possible to contend that the applications performed in this field have already led the chemists to change their way of thinking. For example, the developments recently achieved and allowing chemists to generate in real time the three-dimensional (3-D) molecular structures of unknown compounds and to search for specific 3-D shape properties in large chemical databases are a key step towards the design of new biological active species such as drugs, inhibitors, etc. [1, 2].

In addition to the tremendous progress witnessed recently in hardware and software of visualization tools, MG has also benefited from important methodological developments in computational chemistry. To review just a few, fast and efficient 3-D model builders are now available for both small systems and macromolecules [3]; molecular dynamics methods allow the users to locate the global minimum on complex potential energy surfaces and simultaneously simulate the behavior of molecules in solution as a function of temperature [4]; powerful algorithms have been developed to generate realistic molecular surfaces as solvent accessible envelopes [5] and, last but not least, several approaches have been reported to rapidly evaluate some key local molecular properties such as hydrophobicity, electron densities, electrostatic potentials, reactivity indices, etc. [6, 7]. This latter point is important as these properties can be advantageously displayed on adequate workstations and provide the user with a highly valuable information as to the "hot" regions of a given compound with respect to the approach and possible docking of a specific reactant.

In this context, and just as an example, we have recently developed a quantum chemical procedure to rapidly evaluate the intermolecular interaction energy E_{int} between a substrate S and an incoming reactant R characterized by its electrophilic (i.e., electron acceptor) or nucleophilic (electron donor) behavior [8, 9]. Being a local property representative of a reactivity index, the value of E_{int} may be calculated repeatedly at selected points in the molecular volume of S and visualization techniques allow us to display the results together with the molecular model of S, which leads to an immediate perception of the regioselectivity of the corresponding reaction mechanism (Figure 1).

Figure 1. Solid model of the molecular surface of the ((1,3- dithian-2-yl)cyclohexadienyl)$Cr(CO)_3$- complex colored according to the E_{int} reactivity indexcalculated for electrophilic attack. The most reactive sites correspond to the red zones of the surface. For more details, see ref. [10].

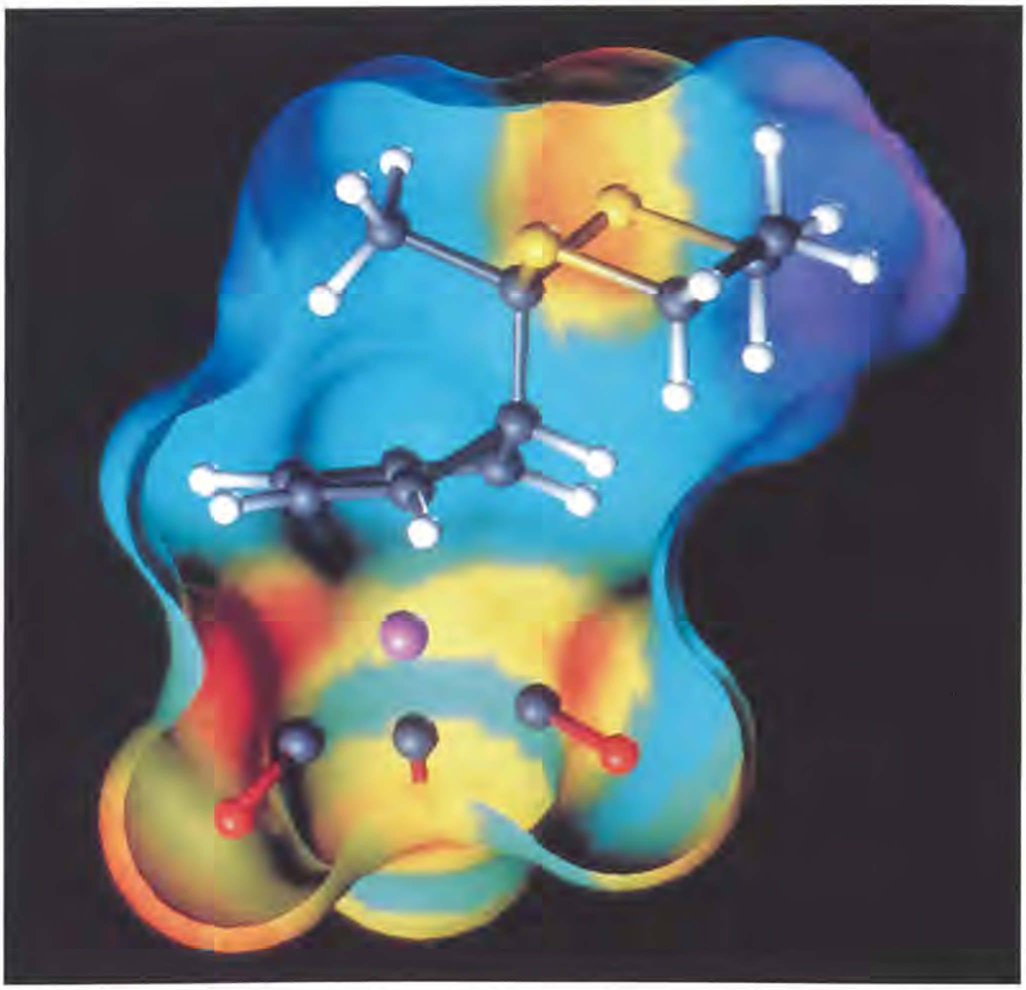

Let us turn to computational quantum chemistry (CQC) which is another essential ingredient of computer-assisted chemistry. The main purpose of CQC is to calculate the electronic energies, wave functions and properties of chemical species using quantum theory. As such, there is no doubt that CQC is also part of molecular modelling, as quantum theory is the best microscopic model to describe the behavior of chemical systems comprising up to 10^3 electrons. However, quantum chemical techniques are notoriously inadequate for modelling macromolecules or solvated systems and one has to turn then to Monte Carlo or molecular dynamics simulations.

The performances of ab initio, or first-principles, CQC methods are today impressive as far as small molecules (up to 20-30 electrons) are concerned: the so-called chemical accuracy (bond distances predicted to within 0.005 Å, enthalpies of formation to within 1 kcal/mol) may be obtained almost on a routine basis by resorting to correlated (post-Hartree-Fock) treatments [11, 12]. However, these techniques, known as MCSCF+CI and many-body perturbation theory [13] in the jargon of quantum chemists, are very expensive in terms of computer time, even though they can take in principle advantage of the vector and multi-tasking facilities provided by supercomputers such as the NEC SX-3. The problem is that these methods scale as N^6 or higher, where N is the number of one-electron basis functions, which immediately underlines their limitations as to the size of the systems to be treated.

On the other hand, it is a well-known feature of CQC that several alternatives to the traditional ab initio methods are available.

The semiempirical techniques present the advantage to scale as N^3, which makes them very convenient to calculate large systems, generally of organic type because of their limited parametrization. However, one may undoubtedly assert that they have definitely found a respected and well-deserved place in the spectrum of CQC tools [14] and that they are largely used in important molecular modelling applications performed in both industrial and academic laboratories.

Another very interesting alternative to the ab initio methods is now provided by density functional theory (DFT) [15]. DFT techniques scale also as N3 and can be advantageously used for large inorganic and organometallic systems, though they are not limited to these. Many DFT applications have been recently reported for a broad range of such compounds and of properties: ground-state geometries, activation energies, dissociation energies, vibrational frequencies, dipole moments, polarizabilities, ionization energies, excitation energies, proton affinities, electrostatic potentials, chemisorption energies, etc. In general, the results are very satisfactory, being at least of the quality of ab initio calculations performed using a large (polarized) one-electron basis set at the MP2 (second-order Moller-Plesset perturbation theory) level, i.e., including a fair amount of electron correlation [16,17].

Finally, we should mention that DFT plays also an important role in molecular dynamics (MD) simulations through the so-called first-principles MD scheme developed recently by Car and Parrinello. In this method, contrary to classical MD procedures based on the use of empirically parametrized potentials, the interatomic forces acting on the atoms of the system investigated are computed, as the simulation proceeds, using electronic structure calculations based on DFT. The interatomic potential is thus parameter-free and derived from first principles, with no experimental input. The Car-Parrinello method has been recently applied to a variety of problems which had previously been inaccessible, such as the determination of the physical properties of disordered systems in their liquid and amorphous states, the investigation of processes relevant to semi-conductor technology, e.g., the diffusion of hydrogen in silicium, as well as the study of surface reconstruction and molecular clusters.

Several DFT and first-principles MD applications are currently performed by our Geneva group on the NEC SX-3 supercomputer, as presented in the following pages, and they have already led to promising modelizations of the structure and properties of materials such as zeolites and semiconductors.

As a conclusion, there is little doubt that the impact of CC on chemistry is going to the steadily growing in the next years, with a spectrum of applications extending progressively to routine modelizations of complex macromolecules and new materials.

References

[1] Ripka, W. C. and J. M. Blaney. "Topics in Stereochem." 20 (1991): 1.

[2] Borman, S. *Chem. Engin. News* 70(32) (1932): 18.

[3] Rusinko, A., J. M. Skell, R. Balducci and R. S.Pearlman. *CONCORD*, University of Texas at Austin, distributed by Tripos Ass., St. Louis, USA (1987).

[4] van Gunsteren, W. F. and H. J. C. Berendsen. *Angew. Chem. Int. Ed. Engl.* 29 (1990): 992.

[5] Connolly, M. L. *Science* 221(1983): 70.

[6] Purvis, G. D. *J. Comp. Aided Mol. Design* 5(1991): 55.

[7] Weber, J. , P. Y. Morgantini, P. Flükiger and A. Goursot. *Visual Computer* 7(1991):, 158.

[8] Daul, C., A. Goursot, P. Y. Morgantini and J. Weber. *Int. J. Quantum Chem.* 38 (1990): 623.

[9] Weber, J., D. Stussi, P. Flükiger, P. Y. Morgantini and E. P. Kündig. *Comments Inorg. Chem.* 14 (1992): 27.

[10] Bernardinelli, G., A. Cunningham, C. Dupré, E. P. Kündig, D. Stussi and J. Weber. *Chimia* 46 (1992): 126.

[11] Curtiss, L. A., C. Jones, G. W. Trucks, K. Raghavachari and J. A. Pople. *J. Chem. Phys.* 93 (1990): 2537.

[12] Bauschlicher, C. W. and S. R. Langhoff. *Adv. Chem. Phys.* 77 (1990): 103.

[13] Hirst, D. M. *A Computational Approach to Chemistry* Oxford: Blackwell (1990).

[14] Zerner, M. C. In *Reviews in Computational Chemistry, Vol. II*, edited by K. B. Lipkowitz and D.B. Boyd, p. 313. New York: VCH, 1991.

[15] Parr, R.G. and W. Yang. *Density-Functional Theory of Atoms and Molecules*. New York: Oxford University Press, 1989.

[16] Andzelm, J. and E. Wimmer. *J. Chem. Phys.* 96 (1992): 1280.

[17] Jungwirth, P., D. Stussi and J. Weber. *Chem. Phys. Lett.* 190 (1992): 29.

Fractional Analysis of Human Lymphocytes and Tumor Cells

G. A. Losa, T. F. Nonnenmacher [a] and G. Baumann

Laboratorio di Patologia Cellulare
Istituto Cantonale di Patologia
Locarno, Switzerland
[a]Abteilung für Mathematische Physik
Universität Ulm
Ulm, Germany

Abstract

Many biological objects appear to have self-similar structures which can be characterized by their fractal dimension D. However, applications of the concept of fractal geometry are rather scarce in cell and tissue biology. Here we have applied a probabilistic method to measure D of membrane boundaries of human lymphocytes recorded by digital processing.

Introduction

Irregular shape, ultrastructural richness and discontinuous morphogenetic patterns connotated tissues, cells and subcellular components which ensure the achievement of peculiar functions and metabolic pathways. A thorough assessment of morphological parameters is of great importance in order to investigate actual connections with biological mechanisms. However, the real shape and the ultrastructural complexity of biological objects are often under-emphasized if not simply disregarded; at best, they are considered as ideal and regular objects. Certainly, this represents a pitfall because facing irregular and complex objects as if they would be regular and smooth may provide unreliable data. To illustrate such a problem suffices to mention the disappointing attempt to compare surface area and volume density estimates of membranes from rat hepatocytes as obtained in different laboratories. [3, 9, 18, 22]. The large discrepancy among estimates could not be explained by differences in handling animals or processing tissues but rather imputable to the skilfulness and length scale (Paumgartner et al, 1981) adopted for measuring membrane details of organelles. Indeed, some papers have clearly indicated that the resolution or the magnification scale at which morphometric measurements are carried out could seriously influence the results about length, surface and other dimensional sizes of biological objects [6, 12, 16]. The reason is that complex and irregular biological objects have fragmented and discontinuous patterns which should be properly described in terms of fractal rather than topological dimensions [10]. However, the euclidean view of geometry is still dominating in morphology and cell biology so that it should not be surprising that the fractal analysis has met with limited applications in biology and medicine [1, 5, 14, 19, 20, 23] and, despite its potentiality, remains practically unexploited in the field of cancer [4, 7]. In the present study, the apparent irregularity of cell surface or plasmalemma of cells isolated from patients with acute lymphoblastic leukemia, of human resting T lymphocytes and of peripheral blood mononuclear cells cultured with mitogenic lectins has been quantified in terms of fractal dimension D with a probabilistic method.

Material and Methods

Resting mononuclear cells isolated by gradient centrifugation from blood samples of normal donors, mononuclear cells cultured in vitro in presence of mitogenic lectins Phytohemagglutinin or Concanavalin A and blast cells isolated from patients with acute lymphocytic leukemia were identified on the basis of the membrane surface phenotype. Cells were stained with fluorescent conjugated monoclonal antibodies directed against surface membrane antigens and measured by flow cytometry (FACSscan, Becton Dickinson). Aliquots of cells from various populations were processed for electron microscopy and micrographs taken with a Philips 400-ET microscope at the magnification of 8000x or 12500x, found well suitable for a complete visualization of single cells. Three different methods of digital image analysis (yardstick, box-counting and probabilistic method) implemented on a parallel version were applied in order to measure the fractal dimension D of cellular profiles. The V. Op. ratio of these three programs was about 70 to 80% at a speed of about 50 MIPS. The taken CPU-time for a run of the yardstick method, was about 7 sec on the NEC SX-3 of CSCS in Manno for a 2048 x 2048 picture.

On a HP 9000, one needs for the same picture about 15 min. The speed up for the two other methods lies between 150 and 170 depending on the size of the picture. Some hundred EM-pictures have been analyzed this way in order to get enough data points for a statistical interpretation. The fractal dimension D of cell perimeter was estimated by applying a probabilistic method exhaustively describe elsewhere [13, 14]. The boundary profile of a cell projected into a plane was picked up by a scanner and the data stored into a memory of a computer in the form of a two-dimensional array. Experimental image analysis is dealing with a geometrical object defined by a set S of points at position $x = (x_1, x_2, \ldots x_E)$ in an E-dimensional Euclidean space. The spatial arrangement of the points determines a probability P(m, ε) stating that there are m points within an E-cube of size centered about an arbitrary point in S. P(m, ε) is directly related to other probability measures as introduced by Mandelbrot. The moment $M_q(\varepsilon)$ of the probability P(m, ε) is defined by

$$M_q(\varepsilon) = \sum_{m=1}^{N} m^q P(m, \varepsilon)$$

where N counts the number of boxes which at least contain one pixel. These $M_q(\varepsilon)$ are related to the fractal dimension D_q by logarithmic derivatives.

Fractal dimensions

Cells	D1	D2	D3	D4	D5	SD+/-
T-lymphocytes (n.d)	1.19	1.20	1.21	1.21	1.22	0.04
T-lymphocytes (CD8+)	1.22	1.23	1.23	1.23	1.23	0.03
T-lymphocytes (CD4+)	1.17	1.16	1.16	1.16	1.17	0.03
PBM (CD3+)	1.20	1.20	1.20	1.20	1.21	0.03
PHA-stimulated PBM	1.11	1.11	1.12	1.12	1.12	0.03
ConA-stimulated PBM	1.25	1.26	1.26	1.27	1.27	0.02

Table 1. Fractal dimensions (five moments) of pericellular membranes from resting and lectin (PHA or ConA) activated lymphocytes. n.d: not decorated with monoclonal antibodies.PBM: peripheral blood mononuclear cells. CD: cluster of differentiation.

Table 2. Fractal dimensions (five moments) of pericellular membranes of lymphoblasts from acute leukemia (ALL) with T or B surface phenotype. CD: cluster of differentiation. n.d: not decorated with monoclonal antibodies.

	Fractal dimensions					
Leukemia type	D1	D2	D3	D4	D5	SD+/-
T-ALL (n.d)	1.10	1.11	1.11	1.11	1.11	0.03
T-ALL (CD2+)	1.12	1.12	1.12	1.12	1.12	0.02
B-ALL (early: n.d.)	1.14	1.14	1.15	1.16	1.18	0.02
B-ALL (n.d)	1.13	1.13	1.13	1.12	1.12	0.03
B-ALL(CD19+)	1.19	1.19	1.19	1.19	1.19	0.03

$$D_q = \frac{1}{q}\left(\frac{d\log M_q(\varepsilon)}{d\log\varepsilon}\right)$$

This particular definition of the probability P(m, ε) has been introduced by Voss and it is very efficient to implement on a computer [21, 2, 14]. The range of ε used in our calculation is spanning three orders of magnitude

$$\varepsilon_{min} \le \varepsilon \le \varepsilon_{max} \text{ with } \varepsilon_{min} = 0.003\mu m \text{ , } \varepsilon_{max} = 3\mu m$$

If all moments give the same value of D_q, then the fractal set is uniform (monofractal) while for a non-uniform fractal set the fractal dimension D_q would take different values indicating that such an object is multi-fractal. We observe (see Tables 1, 2) for each cell line that D_q (q=1, 2, 3, 4, 5) is almost the same within a maximum standard deviation of s.d.=0.06. Hence, we conjecture that very pronounced multi-fractal structures are not present. We finally note that the observed scaling range, i.e., self-similar structures, extends over almost two orders of magnitude, i.e., $\varepsilon_0 < \varepsilon < \varepsilon_1$ with $\varepsilon_0 = 0.012$ μm and $\varepsilon_1 = 3$ μm.

Results

The plasmalemma of peripheral blood CD-3 T lymphocytes and of lymphocytes with suppressor (CD8) or helper (CD4) (Figure 1) phenotype isolated from normal donors, had distinct values within a close interval, i.e., 11.20, 1.233 and 1.17 +/- 1s.d. 0.03, respectively. The fractal dimension was found significantly reduced in T-cells transformed by lectin PHA-stimulation (D=1.12), while increased in ConA-activated T cells (D=1,26) (Table 1). Low D values were recorded on circulating lymphoblasts with distinct surface phenotype and high rate of proliferation, obtained from patients with acute lymphoblastic leukemia (ALL). T-ALL blasts had a characteristic mean D of 1.11-1.12 (Figure 2) while B-ALL and early -B-ALL blasts had mean D values of 1.113 and 1.16 respectively, suggesting that the latter leukemic cells with less mature B immunphenotype had surprisingly a surface profile somewhat less smooth than B-ALL blasts (Table 2). Applications of the fractal concept in stereology are traditionally based on the perimeter scaling law $L(\varepsilon) = \varepsilon^{\alpha}$, which yields -- beside the fractal dimension D--additional structural information [15]. Figure 4 shows a log $L(\varepsilon)$ versus log (ε) plot for two magnification of a hairy leukemic cell (Figure 3). The slope α of the straight line indicating self-similar structure is related to D by $D = 1- \alpha$. The data points represent our numerical results for the perimeter $L(\varepsilon)$ of one and the same contour of a hairy leukemic cells taken by two different magnifications (8700x, 18400x). The slope α of the straight line is found to be α=-0.34, leading to D=1.34. This dimension is far beyond the dimension of T-lymphocytes as expected. In fact, just by visual inspection of EM-picture (Figure 3) more wiggliness or roughness of a hairy leukemic cell contour can be seen with respect to the cell boundary of a normal T-lymphocyte. Computerized image analysis, as used here yields a reproducible and consistent number for

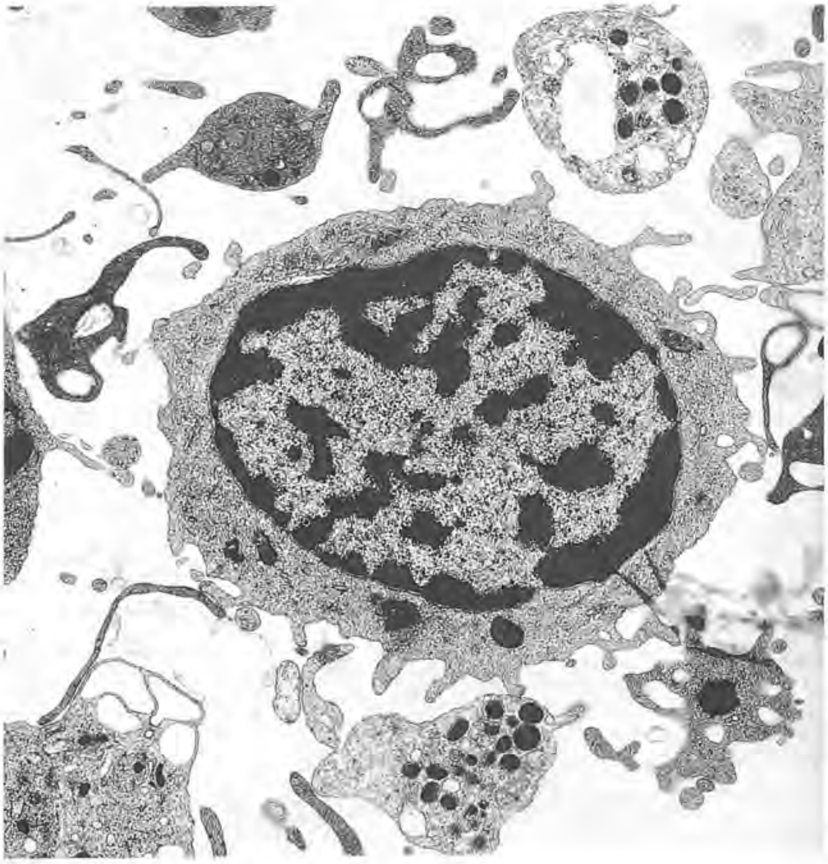

Figure 1. Electron microscopy view of a resting T-lymphocyte isolated from blood of a normal donor. Surface microvilli and irregularities can be seen. Magnification 18400 x.

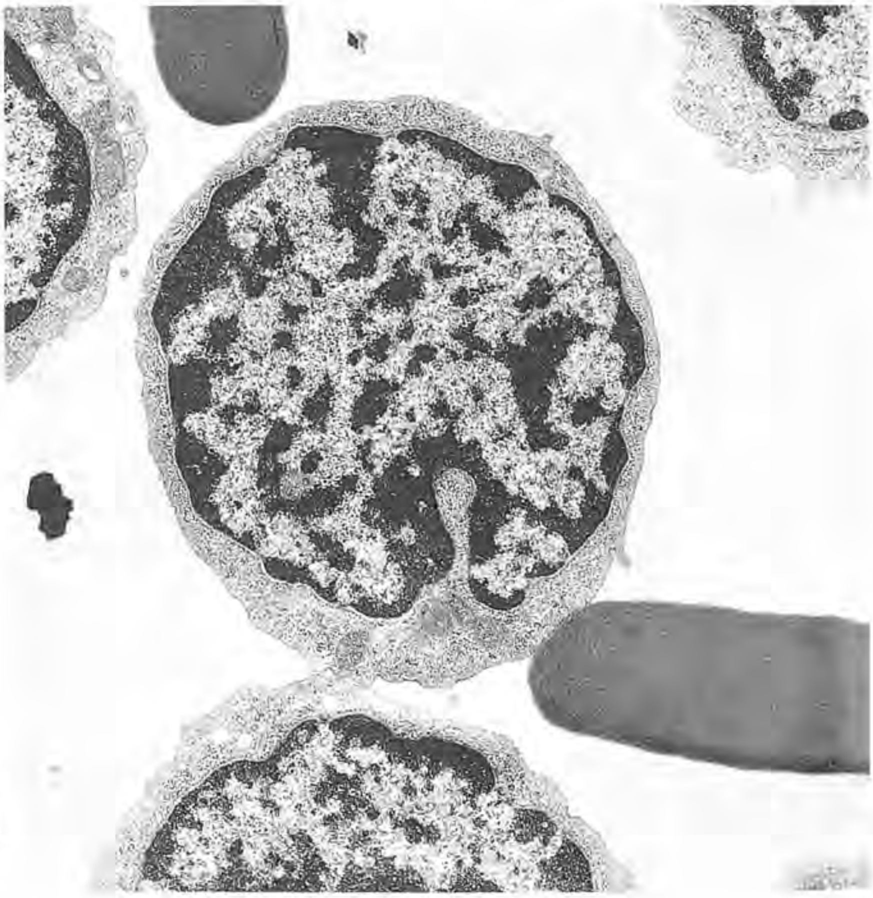

Figure 2. Electron microscopy view of a T-leukemic cell (T-ALL), characterized by a smooth membrane contour. Magnification 18400x.

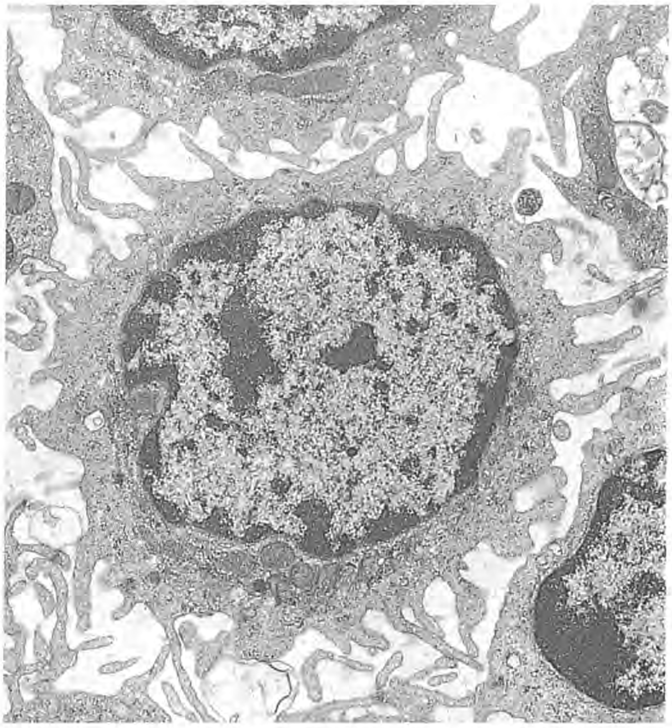

Figure 3. Electron microscopy view of a hairy leukemic cell characterized by a rough membrane contour. Magnification 18400x.

the parameter D free of any subjective influence. Besides the dimension D, note that for small ε-values the perimeter $L(\varepsilon)$ reaches a saturated value (plateau) L_{max}. The plateau value depends on the magnification M. For $M = M_1 = 18400x$ the maximum value is given by $L_{max} = L(M_1) = 60.8\ \mu m$ (upper curve), and for $M = M_2 = 8700x$ we find $L_{max} = L(M_2) = 53.1\ \mu m$ (lower curve). Additionally we observe that the higher magnification the larger the ε-span that follows the straight line, i.e., the higher the magnification the more structural details of the contour are observable and thus resulting into a larger domain of self-similar structure.

Discussion

Hematopoietic cells, like lymphocytes and peripheral blood mononuclear cells isolated from normal human donors, lectin stimulated T-cells and lymphoblasts from acute lymphoblastic leukemia manifest a self-similar behavior and a characteristic fractal dimension of cell periphery. The fractal concept which was applied for the first time to human normal and leukemic blood cells, required only one parameter, the fractal dimension D, in order to characterize the contour irregularities, in contrast to other more familiar concepts based on an approximation of the contour-curve by a polynomial expansion which needs a huge number of fit parameters [17]. Substantially, this study indicated that lymphoblasts raised in vitro by lectin stimulation of a normal mononuclear cell population or blasts from leukemic origin are proliferating cells whose plasma membrane had an irregular profile with a D value significantly different from that found on normal mature blood T-cells. Both types of blasts, either of leukemic origin or raised by in vitro stimulation with PHHA or ConA displayed T surface antigens. The physiopathological meaning and the biochemical mechanisms inherent the observed changes of irregularity on the plasma membrane of leukemic and in vitro proliferating blasts are not well understood as yet. It might be related to modifications in the configuration and composition of membrane lipids induced by mitogenic and/or neoplastic factors and, at least in leukemic cells [8], to the enhanced shedding of membrane fragments from the cell surface. Another relevant point concerned with the finding that lymphocytes and lymphoblasts as well had a uniform characteristic fractal dimension D. Indeed, we could not observe a great difference of D among the five moments of order q for a given cell type and within an estimated error of less that 10%, which excluded any multi-fractal structure. The fractal dimension alone does not completely define the cellular shape nonetheless it is a quantitative descriptor which distinguishes contour properties and in combination with other measures might allow ultrastructural and antigenic features to be correlated with biochemical and dynamical processes underlying the plasma membrane of mature lymphocytes and tumor cells.

Acknowledgments

This investigation has been supported by the Swiss National Science Foundation, No. 31-25702.88. We also acknowledge gratefully support by the Swiss Scientific Computing Center in Manno (CSCS) for making available to us their computer equipment.

References

[1] Barnsley, M. *Fractals Everywhere*. Boston: Academic Press, 1988.

[2] Baumann, G. and T. F. Nonnenmacher. "Determination of fractal dimension." pages 93-104 in *Gli oggetti frattali in astrofisicia, biologia, fisica e matematica*, edited by G.A. Losa, D. Merlini and R. Moresi. Locarno: Cerfim, 1989.

[3] Bolender R.P., D. Paumgartner, G.A. Losa, D. Muellener and E.R. Weibel. "Integrated Stereological Biochemical Studies on Hepatocytic Membranes. I. Membrane Recoveries in Subcellular Fractions." *J. of Cell Biol.* 77 (1978): 565-583.

[4] Caldwell, C.B., S.J. Stapleton, D.W. Holdsworth, R.A. Jong, W.J. Weiser and Yaffe M.J. Cooke. "Characterization of Mammographic Parenchimal Pattern by Fractal Dimension." *Phys. Med. Biol.* 35 (199): 235-547.

[5] Goldberger, A.L., V. Bhhargava, B.J. West and A.J. Mandel. "On a Mechanism of Cardial Electrical Stability." *Biophys. J.* 48 (1985): 525--528.

[6] Keller, H.J., H.P. Friedli, Pl. Gehr, M. Bachofen and E.R. Weibel. "The Effect of Optical Resolution on the Estimation of Stereological Parameters." In *Proceedings, Fourth International Congress on Stereology*, Gathersburg, U.S.A. (1976): 409-431; U.S. Department of Commerce, National Bureau of Standards, Special Publications.

[7] Losa, G. A. "La dimensione frattale nell'analisi morfometrica delle ultrastruttuure." *Microscopia Elettronica* 12 (1991): 118-126.

[8] Losa, G., A. D. Heumann, S. Carrel, V. von Fliedner and J.P. Mach. "Characterization of Membrane Visicles Circulating in the Serum of Patients with Common Acute Lymphoblastic Leukemia." *Lab. Invest.* 55 (1986): 5733-579.

[9] Loud, A.V. "A Quantitative Stereological Description of the Ultrastructure of Normal Rat Liver Parenchymal Cells." *J. of Cell Biol.*37 (1968): 27-46.

[10] Mandelbrot, B.B. *The Fractal Geometry of the Nature*. San Francisco: Freeman, 1982.

[11] Nonnenmacher, T.F. "A Scaling Model for Dichotomous Branching processes." *Biol. Cyber* 56 (1987): 155-159.

[12] Nonnenmacher, T.F. "Fractal shapes of Cell Membranes and Pattern Formation by Dichotomous Branching Processes." In *Thermodynamics and Pattern Formation in Biology*, edited by I. Lamprecht and A.I. Zotin. Berlin-New York: Walter de Gruyter, 1988: 371-394.

[13] Nonnenmacher, T.F. "Fractal Structures in Biomedical Systems and Morphogenetic Scaling Processes." In *Gli oggetti frattali in astrofisicia, biologia, fisica e matematica* edited by G.A. Losa, D. Merlini and R. Moresi. Locarno: Cerfim,1989: 64-92.

[14] Nonnenmacher, T.F., G. Baumann and G.A. Losa. "Self-organization and Fractal Scaling Patterns in Biological Systems." In *Trends in Biological Cybernetics* edited by J. Menon. Publications Manager, Research Trends, Council of Scientific Research Integration, Trivandrum India, 11 (1990): 65-73.

[15] Nonnenmacher, T.F. "Structural Analysis of Cell Profiles and Fractional Dynamic Processes." In *Fractals in Biology and Medicine*, edited by G. A. Losa, T.F. Nonnenmacher and E.R. Weibel. Basel: Birkhäuser Verlag (to appear).

[16] Paumgartner, D., G.A. Losa and E.R. Weibel. "Resolution Effect on Stereological Estimation of Surface and Volume and its Interpretation in Terms of Fractal Dimensions." *J. Micros.* 121 (1981): 51-63.

[17] Pesce-Delfino, V., F. Potente, E. Vacca, T. Lettini, P. Ragone and R. Ricco. "Shape Evaluation in Medical Image Analysis." *Eur. Micros Anal.* 7 (1990): 212- 224.

[18] Reith, A. "The Influence of Triiodothyronine and Riboflavine Deficiency on the Rat Liver with Special Reference to Mitochondria. A morphologic, morphometric and cytochemical study by electron microscopy." *Lab. Invest.* 29 (1973): 216-227.

[19] Smith, TG. , M.B. Marks, G. D. Lange, W.H. Sheriff Jr. and E. A. Nearle. "A Fractal Analysis of Cell Images." *J. Neurosc. Meth.* 27 (1989): 173-180.

[20] Stöber, W. "Dynamic Shape Factors of Non-spherical Aerosol Fine Particles." In *Assessment of Airborne Particles.* Springfield, Illinois: Charles C. Thomas Publishers, 1972: 90-102.

[21] Voss, R.F. "Random Fractals: Characterization and Measurements." In *Scaling Phenomena in Disordered Systems*, edited by R. Pynn and A. Skjeltrop. New York: Plenum Press, 1985: 1-11.

[22] Weibel, E.R., Stäubli, H.R. Gängi and F. A. Hess. "Correlated Morphometric and Biochemical Studies on the Liver Cell. I. Morphometric Model, Stereologic Methods and Normal Morphometric Data for Rat Liver." *J. Cell Biol.* 42 (1969): 68-91.

[23] Weibel, E.R. "Fractal Geometry: A Design Principle for Living Organisms." *Am. J. Physiol.* 261 (1991): L361-L369.

Structure and Dynamics of Proteins in Solution

W. Braun, B. von Freyberg, M. Billeter, P. Güntert, P. Luginbühl,
V. Dötsch, G. Wider and K. Wüthrich

Institut für Molekularbiologie und Biophysik,
ETH Zürich,
Zürich, Switzerland

The aim of this project is to support experimental investigations of the three-dimensional structure and dynamics of proteins in aqueous solution. This involves the development of efficient algorithms and software packages for the processing of complex NMR spectra, spectral analysis, and structure calculations from NMR data. The calculations done at the NEC SX-3 in 1992 dealt specifically with the efficient processing of NMR data with the new software package PROSA, complete relaxation matrix refinement of protein structures with the program DIANA, and novel procedures to refine proteins in water with the program packages FANTOM and OPAL.

Multi-dimensional nuclear magnetic resonance experiments for the determination of protein structures in solution yield large data sets: the signal is measured as a function of several time coordinates and has to be transformed into a multi-dimensional frequency-domain spectrum for the analysis. For efficient execution of the necessary steps such as linear prediction, digital filtering, Fourier transformation, automatic phase correction, and baseline correction a high computation speed and 100-500 Mbyte of memory is required. For this purpose we developed the new software package PROSA [1] that is especially optimized for the architecture of the NEC SX-3. We completely vectorized the time-consuming routines and reduced the input/output operations to a minimum by using the large memory of the NEC SX-3. The program PROSA achieves (including input/output) a computation speed of 300-500 MFLOPS, and needs about 100 times less CPU time than comparable, commercial programs written for use with scalar computers. This makes it possible to routinely use more sophisticated methods than Fourier transformation for signal analysis.

After the first stage of a three-dimensional structure determination by distance geometry calculations, the structures can be refined by a non-linear least squares fit calculation to the measured NOE intensites. We have implemented a complete relaxation matrix refinement procedure in our distance geometry program DIANA. This new method analytically calculates derivatives of the target function. The most time consuming parts are matrix multiplications and the calculation of the eigenvectors and eigenvalues of large matrices in each optimization cycle.

The large memory of the NEC SX-3 allows to calculate and store intermediate quantities. A specially adapted version of the DIANA program for the NEC SX-3 needs 6.7 sec of CPU time per iteration cycle for a protein with about 60 amino acid residues. This corresponds to a computational speed of 500 MFLOPS, which makes this refinement procedure attractive for use with proteins.

The inclusion of water molecules in the energy refinement or molecular dynamics calculations of proteins still represents a computational challenge even for the power of supercomputers. We have included an energy term representing the protein-water interaction in our energy refinement and Monte Carlo simulation package FANTOM [2]. For this energy term the surface areas of the individ-

Space filling representations of four structures of the a-amylase inhibitor calculated by FANTOM on the NEC SX-3 including different energy surface terms. Colour code: red for residues with negative charge, blue for residues with positive charge, yellow for polar, and light-blue for nonpolar residues.

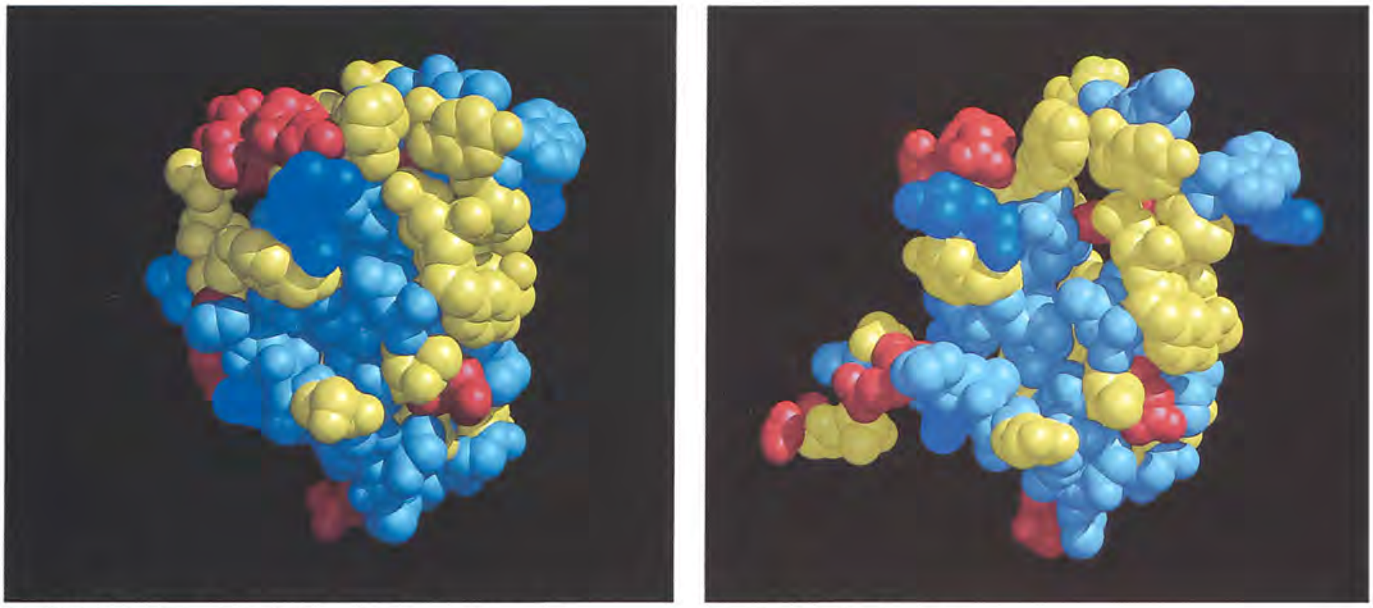

(a) NMR structure in solution used as a reference structure. The other three structures are calculated with different energy surface terms

(b) minimization in vacuo

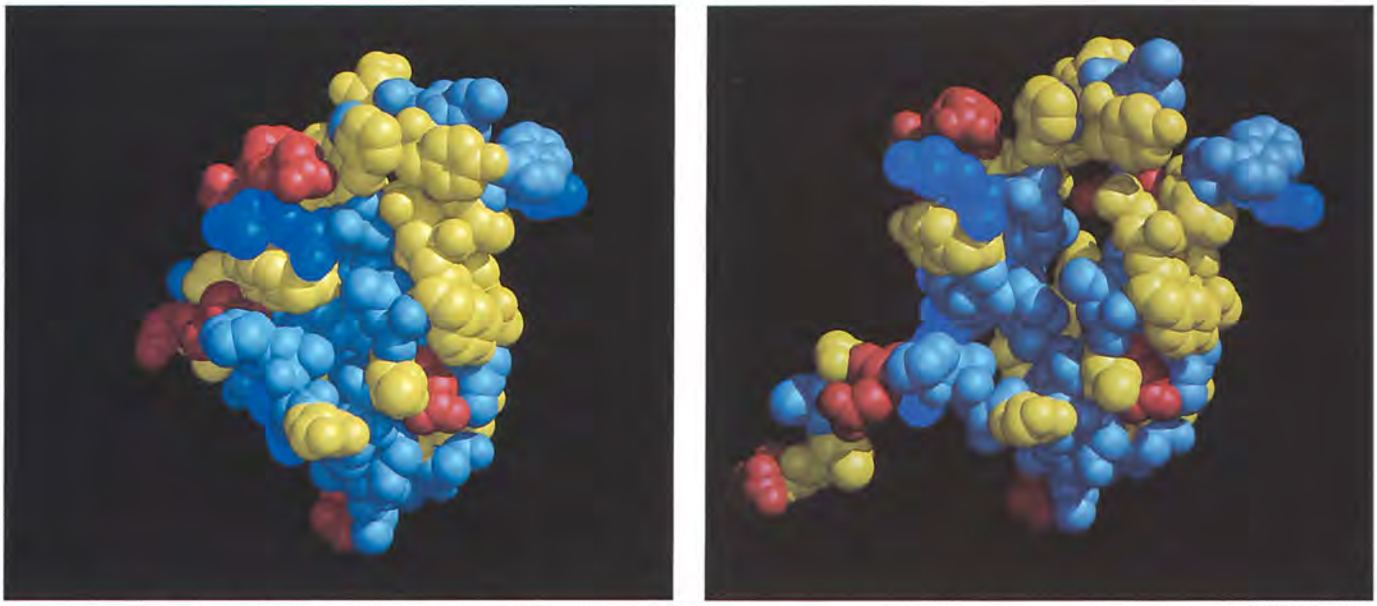

(c) minimization of the total accessible surface area

(d) minimization using the Wesson-Eisenberg parameter set.

ual atoms accessible to the solvent are calculated and used with empirical atomic solvation parameters to estimate the contribution of the solvent. Extensive calculations on the NEC SX-3, starting from 25 different initial conformations of the a-amylase inhibitor Tendamistat and using four different atomic solvation parameter sets, showed that simple parameter sets derived from packing considerations provide a better driving force towards the NMR structure in aqueous solution than more sophisticated parameter sets published in the literature [3]. The structure calculated without NMR constraints but minimizing the total accessible surface area, closely resembles the NMR structure, which is in contrast to the structure obtained by minimization in vacuo, or with the Wesson-Eisenberg parameter set (see figure).

Our program OPAL is used for energy minimizations and for simulations of molecular dynamics of proteins or molecular complexes with proteins. In contrast to generally available programs such as AMBER, the new program OPAL allows the recording of parameters, that correspond to NMR data, as a function of the simulation time. Other data such as relaxation times offer relations between the force field used in the simulation and the NMR experiments.

Furthermore, the new program is designed to make optimal use of the NEC SX-3 hardware. Already during short minimizations this allows MFLOPS-rates of nearly 700 (this average value includes all steps of the program, e.g., also input and output procedures). The high degree of vectorization was achieved by omitting the use of distance cutoffs. This warrants a precise description of all interatomic interactions even when the protein is immersed in a water bath. Initial applications show that OPAL proceeds with the minimization until very low values of the gradients are obtained (to be published).

List of Publications

(based on computations performed with the NEC SX-3)

[1] Güntert, P., V. Dötsch, G. Wider and K. Wüthrich. *J. of Biomol.* NMR (1992) in press.
[2] von Freyberg, B. and W. Braun. *J. of Computational Chem.* (1992) in press.
[3] von Freyberg, B., T.J. Richmond and W. Braun. (submitted).

Material Sciences

Modeling of Polymeric Systems

J. J. de Pablo[1], M. Laso, E. Leontidis, U.W. Suter and A. Widmann
Institut für Polymere
ETH Zürich
Zürich, Switzerland

The goal of modeling in polymer science is to gain a better understanding of polymeric materials and their macroscopic properties with the help of microscopic models. In the research projects described in this report, almost all modeling is conducted in atomistic detail (see accompanying figure) with the hope that in this way the use of adjustable parameters can be avoided. Such modeling techniques provide a wealth of information on polymeric matter and make it possible to describe amorphous and crystalline polymers and their properties with greater sophistication that is possible with more traditional methods.

The characterization of polymeric materials at the molecular level is one of the major goals of materials science. Ideally, one would like to be able to predict a wide range of thermodynamic, structural, dynamic, and mechanical properties of a polymeric material starting from the structure at the molecular level. One would also like to be able to predict the variation of material properties upon chemical modifications at the molecular level, and to be able to design new materials with desired properties using computer-generated information. The research effort in our group is concentrated on the development of statistical- mechanical methods for the simulation of dense polymer phases.

Under the generic name of statistical-mechanical methods, several lines of research have been pursued with the common objective of simulating dense, atomistically detailed polymer systems. The main goal is the development of efficient Monte-Carlo methods for the representative sampling of NVT, NPT and Gibbs statistical mechanical ensembles. Three major available polymer simulation methodologies are available, namely Molecular Mechanics, Molecular Dynamics, and Monte Carlo. Molecular Mechanics is appropriate for the study of mainly static properties, although in certain cases it can provide important dynamic information. The scope of Molecular Dynamics is rather limited, since in dense polymers many important dynamic processes occur at time scales much longer than the maximum time length that can be simulated by Molecular Dynamics. Monte Carlo methods are more flexible, since they can sample the configuration space under investigation in drastic ways. Monte Carlo moves may be preferentially biased towards certain degrees of freedom that provide maximum change of the information content per move, while Molecular Dynamics treats all the degrees of freedom of the system on an equivalent basis. Monte Carlo algorithms do not contain explicit real-time information, but they can in principle be calibrated to provide dynamic information. Phase equilibria of chain molecules and solubility of low molecular weight compounds in long-

---

[1] currently at the Department of Chemical Engineering, Madison

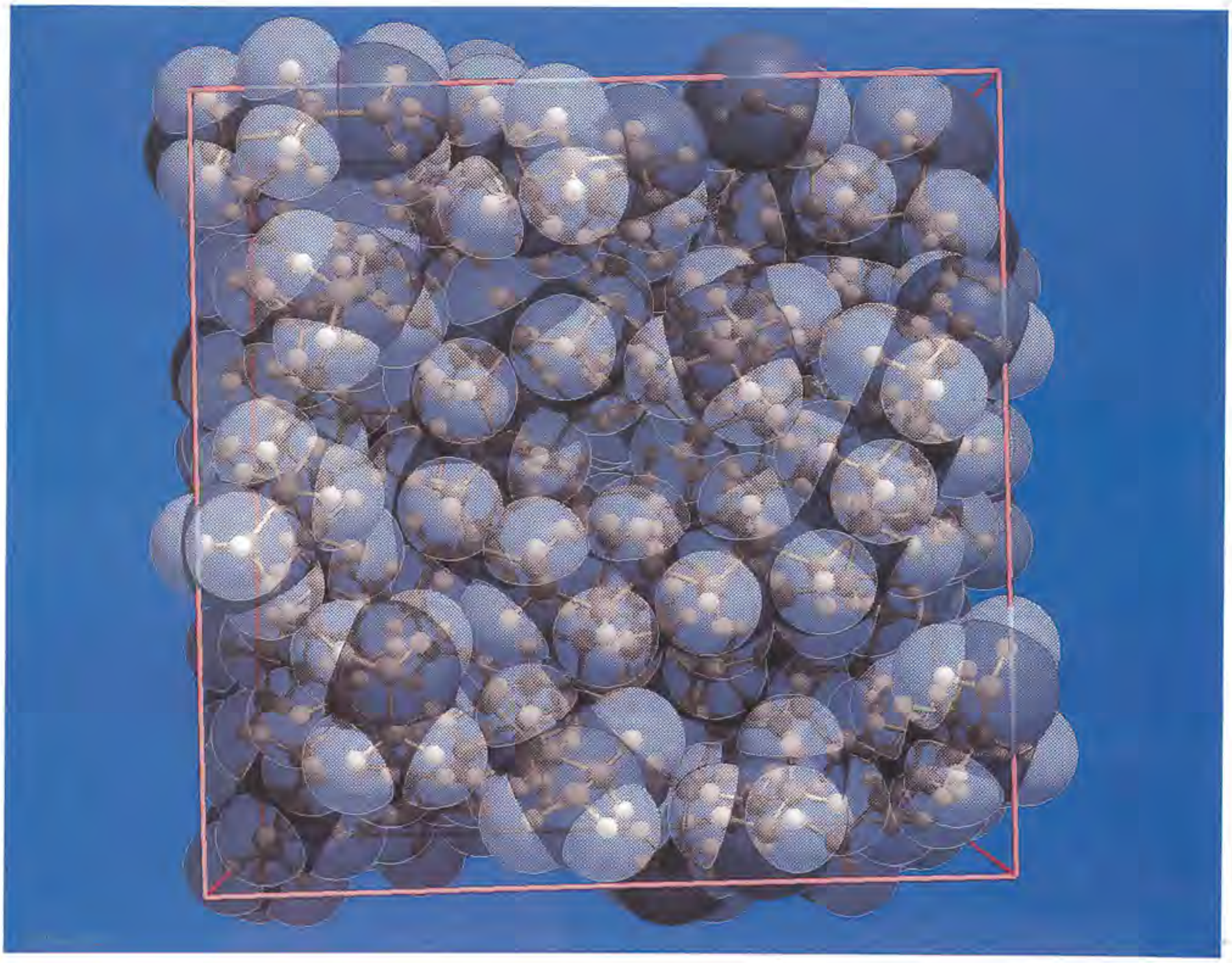

chain molecular systems could be calculated in our group by means of the Continuum Configurational Bias (CCB) MC developed. Additionally, novel composite algorithms for efficient off-lattice simulations of dense polymer phases have been implemented in the case of polyethylene in the united and explicit atom approximations. The medium-term research goal is to generate new powerful Monte Carlo algorithms that (i) are capable of efficiently simulating dense phase of long-chain polymers with realistic chemical structures, and (ii) can be calibrated in an unambiguous manner to provide dynamic properties. In their initial (design) stage, these novel algorithms will be applied to the melt phase of polyethylene, but will subsequently be generalized to treat melts, glasses, and rubbers of chemically realistic polymers, such as polypropylene, polycarbonate, and polystyrene.

The Continuum-Configuration Bias method (CCB) is a novel powerful Monte Carlo method that was developed by this group, based on similar algorithms developed for lattice models or for idealized chain models. It is useful in a number of important applications, such as polymer phase equilibria, studies of solubility of small molecules in polymers, investigation of PVT behavior and thermodynamic properties of polymers. Simulations have been carried out in the canonical, the NPT, and the Gibbs ensemble. Algorithms are already available for the treatment of melts of polyethylene, polypropylene and polystyrene. The CCB method has recently been combined with the Concerted Rotation method (CONROT), which is a novel method for the Monte Carlo simulation of polymers. Extensions of the CONROT move combined with CCB have provided what we believe to be the most powerful currently available Monte Carlo algorithm for the off-lattice simulation of dense polymer phases. The composite simulation method that we have developed will be applied to the study of thermodynamic properties of realistic polymers, such as polypropylene and polystyrene. The glassy state will be simulated, with emphasis on the approach to the glass transition temperature to obtain improved understanding of the way that material properties change as we approach the glass transition temperature both from lower and from higher temperatures.

Tracer diffusion is also studied both in the melt phase and in the glass. We believe that the Monte Carlo methods that we have developed can be calibrated to examine the diffusion of both small spherical molecules in the glass, and of small spherical molecules and longer flexible molecules in the melt. If the techniques allow it, we aim to study plasticizer diffusion in solid polymers. The study of plasticizer diffusion will open a new exciting possibility for the application of computer simulation to polymer technology. At the same time, novel Monte Carlo methodologies will be

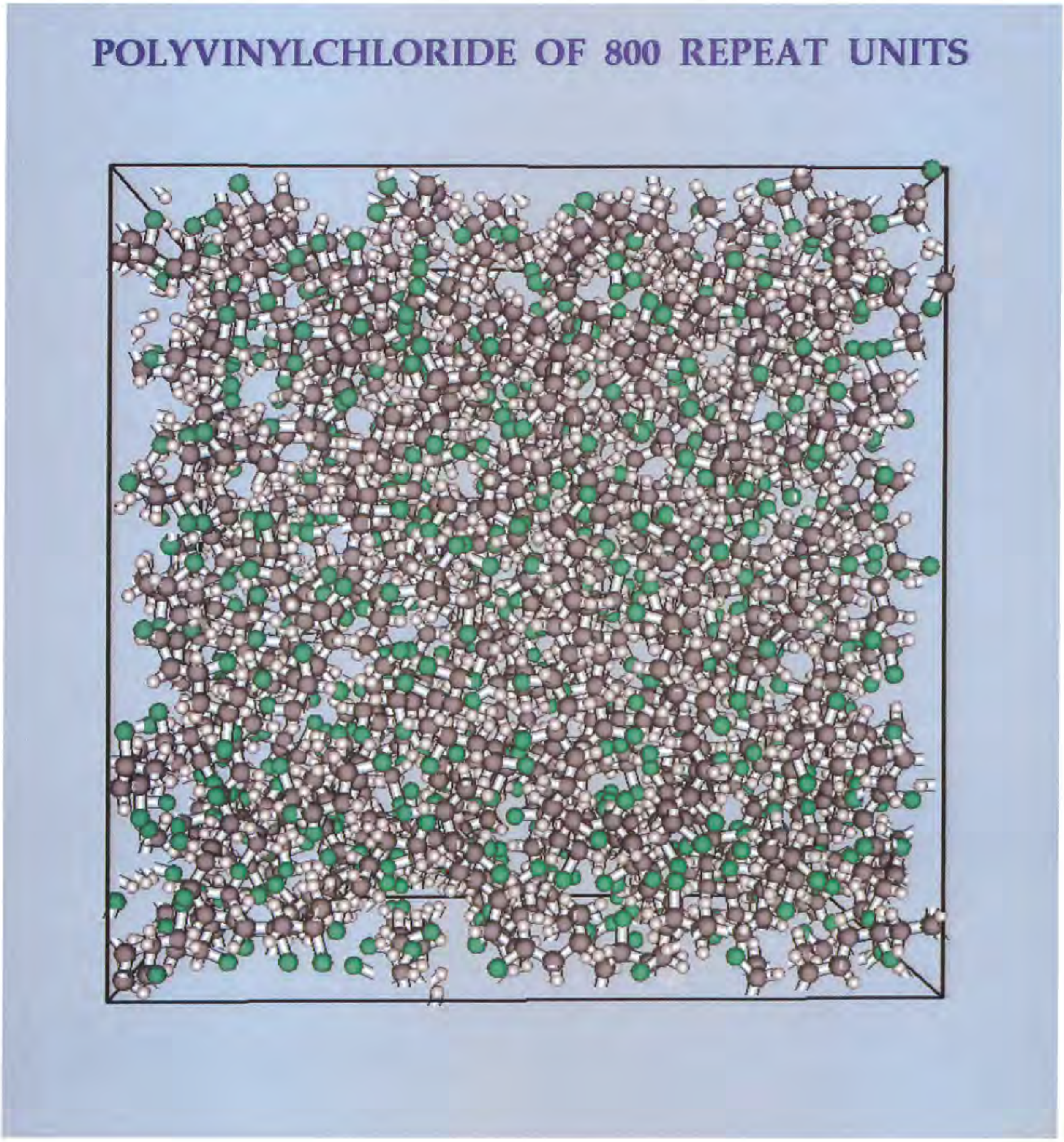

developed. Based on existing Force-Bias and Smart Monte Carlo methods for spherical atoms a Dynamic Monte Carlo algorithm for polymers was recently developed by this group. Preliminary results obtained indicate that this alternative algorithm is very promising for the study of thermodynamic and dynamic polymer properties. The Dynamic Monte Carlo algorithm will be extended, incorporating Fourier acceleration methods that were recently developed for the efficient sampling of near critical systems. It is anticipated that this new algorithm will have unique dynamic properties, and will provide an important new tool in the area of computer simulation of polymers.

The simulation algorithms are based on combinations of traditional methods with recently developed Monte Carlo moves. Complex systems, for which individual methods fail, can be studied conveniently using these algorithms. The classical Metropolis Monte Carlo (MMC) and Reptation methods (REPT) are supplemented with the Continuum Configurational Bias (CCB), and the Concerted-Rotation (CONROT) methods. Many extensions of the CONROT method, involving the simultaneous coordinated displacement of four to seven chain backbone sites, are currently under development. Concerted-Rotation based methods enhance the performance of the algorithm at the level of local segmental motions, whereas the CCB component is important for the convergence of global properties, such as the relaxation of end-to-end distance vectors. The present composite algorithm constitutes the most promising currently available tool for the off-lattice simulation of realistic models of polymer melts and glasses. A satisfactory treatment of relatively long polymer chains (with more than 50 carbon atoms in the backbone) is now possible at experimental melt densities, both in the NVT an NPT ensembles. The NEC SX-3 played a crucial role in many of the calculations performed in this project and very especially in the simulation of phase equilibria.

List of Publications

[1] de Pablo, J. J., M. Laso and U. W. Suter. *J. of Chem. Phys.* 96(3) (1992): 2395.
[2] de Pablo, J. J., M. Laso and U. W. Suter. *J. of Chem. Phys.* 96(8) (1992): 6157.
[3] Laso, M., J. J. de Pablo and U. W. Suter. *J. of Chem. Phys.* 97(4) (1992): 2817.
[4] de Pablo, J. J., M. Laso and U. W. Suter. *Siepmann Molecular Physics* (in press, 1992).

Realistic Modelling of Materials by Quantum Simulations

**F. Ancilotto [a], R. Car [b, c], F. Kirchhoff [b], G. Galli [b], L. Gilgien [b],
F. Mauri [b], E. Moroni [b], A. Pasquarello[b, d], J. Sarnthein [b, e],
O. Sugino [b, f], F. Tassone[b, g] and A. Vittadini [h]**

[a] Department of Physics
University of Padova
Padova, Italy

[b] Institut Romand de Recherche Numérique en Physique Matériaux (IRRMA)
PHB-Ecublens
Lausanne, Switzerland

[c] Department of Condensed Matter Physics
University of Geneva
Geneva, Switzerland

[d] AT&T Bell Laboratories
Murray Hill, NJ U.S.A.

[e] Institute of Electrochemistry
Technical University of Vienna
Vienna, Austria

[f] NEC Fundamental Research Laboratory
Tsukuba, Japan

[g] Scuola Normale Superiore
Pisa, Italy

[h]Department of Chemistry
University of Padova
Padova, Italy

Ab-initio molecular dynamics (MD) simulations allow to move atoms under the action of forces that are derived directly from the instantaneous electronic ground-state. In this way the subtle interplay between atomic motion and evolution of chemical bonds is accurately taken into account, resulting in a significant predictive power. This approach has been applied to study a variety of systems and processes of interest in material science such as diffusion processes in silicon, adatom migration on the silicon surface, hydrogen etching of the silicon surface, diamond surface re construction, and disordered silicon-carbon alloys. New algorithmic advances developed at IRRMA have extended the application of ab-initio MD techniques to elements with tightly bound electrons, such as oxygen in water and transition metal systems.

The computational facilities of CSCS and particularly the NEC SX-3 have allowed to accomplish the following results:

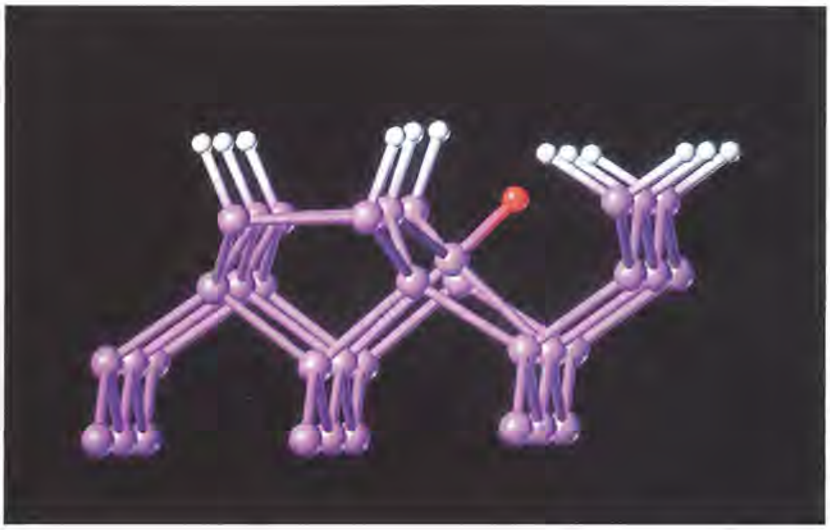

Figure 1a. Equilibrium atomic configuration for an excess H atom adsorbed on the hydrogenated Si(100) 3 x 1 surface. Violet and white spheres are used to represent silicon and hydrogen atoms of Si(100) 3 x 1, respectively, while the excess H atom is shown as a red sphere. Atoms of the topmost four layers and three (3 x 1) surface unit cells are shown.

Hydrogen Etching of the Si (100) Surface

A process of great current interest in surface physics is atomic corrosion, or etching, which may occur when an element present in gaseous phase reacts with the surface atoms. For instance, when atomic hydrogen interacts with the silicon surface, stable silane (SiH_4) molecules may be formed and desorbed from the surface. The rate of this reaction, which occurs at large H exposures, is found to be particularly high for the Si(100) surface, presumably due to the prominent Si backbonds on this surface [0, 0, 0]. On the (100) terraces the etching process is likely to be initiated by the rupture of one of the Si-Si backbonds, leading to the formation of an adsorbed silicon trihydride ($SiH_3(a)$) species, and subsequently (after breaking of another silicon bond) of gaseous SiH_4.

Recently, the Car-Parrinello method has been used to investigate the process of silicon backbond breaking [1]. In these calculations periodically repeated systems containing up to 144 Si and 98 H atoms were treated, and the determination of optimal structures was achieved via simultaneous relaxation of ionic and electronic degrees of freedom. As a first step, the adsorption of an excess H atom on a hydrogenated Si(100) surface consisting of an ordered "3 x 1" arrangement of monohydride and dihydride units was considered. Among a number of possible H-adsorption sites, anti-

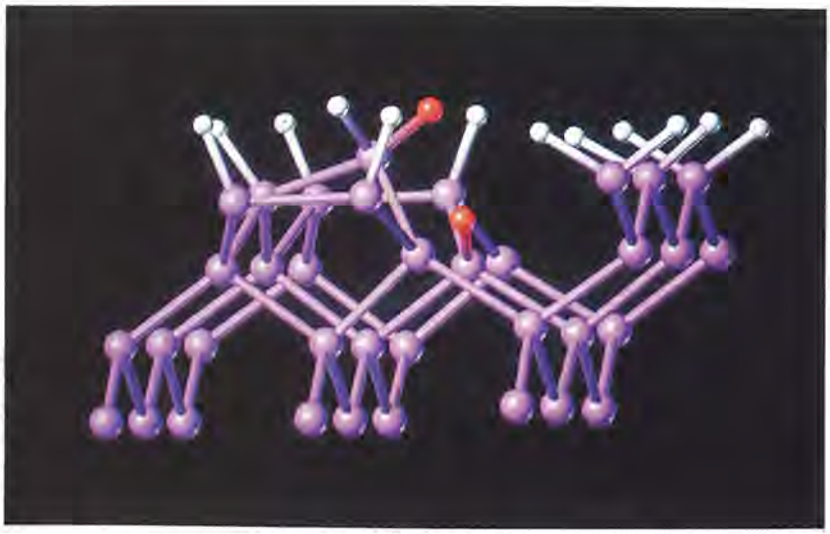

Figure 1b. Equilibrium atomic configuration after a second H atom (also shown as a red sphere) has reached the surface (see text). The breaking of one of the backbonds connecting a surface silicon atom to the second layer is apparent.

bonding (AB) sites of the bonds between 2nd and 3rd layer atoms, close to the 2nd layer atoms, were found to be energetically favored. The calculated fully relaxed structure of a H adatom in such an AB_2 site is shown in Figure 1a.

The presence of a H-adatom at the AB_2 site weakens the bonds of the neighboring Si atom, which can therefore be attacked very effectively by other H atoms approaching the surface. This has been explicitly seen in a numerical simulation where, starting from the state in Figure 1a, the adsorption of a second excess hydrogen was considered. This second H atom was let approach the surface close to the Si surface dimer atom on the left of the H adatom in the AB_2 site. A radical change of the local atomic structure started immediately to develop, accompanied by corresponding changes in the bonding configuration. The resulting fully relaxed structure is shown in Figure 1b. Here it appears clearly that the dimer backbond is broken, and has been replaced by two SiH units formed by the Si dimer and 2nd layer atoms with the two excess H adatoms. The strong displacements of the various atoms involved in the reaction from their original positions are also evident. Thus the picture which emerges from these calculations is that the H-induced rupture of Si-Si backbonds is a two-step process as shown in Figure 1a+1b, i.e., the state with one H adatom adsorbed at AB_2 acts as a precursor to the bond breaking reaction.

Liquid Transition Metals: l-Cu.

In noble and transition metals the *d*-orbitals play an important role in the bonding properties and must be included among the valence wave functions in an accurate description. The localized nature of the *d*-orbitals, particularly the 3*d*, requires a very large number of basis functions in a plane wave expansion. This has until recently prevented large scale first-principles MD simulations of noble and transition elements. Recent algorithmic advances [0, 0, 0] have allowed to overcome this difficulty and made it possible to simulate a *d*-bonded liquid metal, such as *l*-Cu [2].

Liquid Cu has been simulated by a system of 50 Cu atoms in a periodically repeated simple cubic box. The density of Cu atoms has been taken to be the experimental one at the melting temperature ($\rho = 7.97$ g/cm^3 at $T_M = 1356$). During a run of 2 ps various quantities could be measured, such as the pair correlation function, the self-diffusion coefficient, and the electronic density of states. The pair correlation function gives the average particle distribution measured as a function of distance from a tagged atom. Experimentally it can be extracted from the scattering intensities obtained from x-ray or neutron diffraction data. In Figure 2 the computed pair correlation function of *l*-Cu is com-

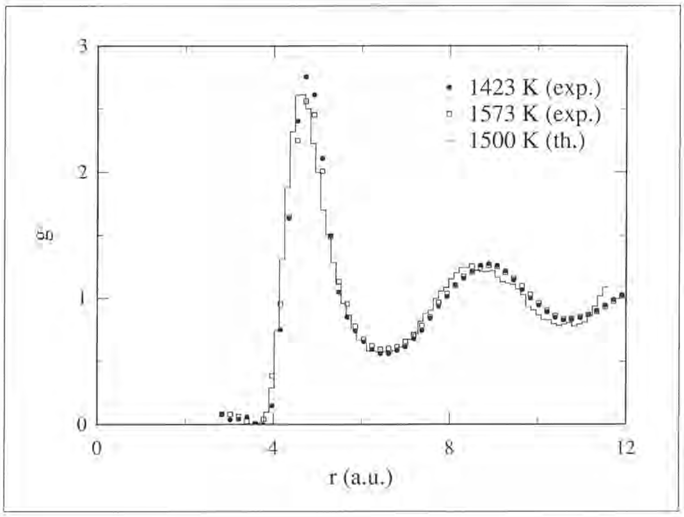

Figure 2. Radial pair correlation function for *l*-Cu. The histogram is obtained from the MD simulation of Ref. [11]. Experimental data are taken from [13]. The temperatures corresponding to MD simulation and experiments are reported in the inset. From Ref.[2]

pared with experiment, showing excellent overall agreement. It should be stressed that the only pieces of empirical information used to set up the computer experiment are the atomic number for copper and the macroscopic density. This illustrates the kind of accuracy and the predictive power that can be achieved with such simulations.

This study of liquid Cu shows that nowadays it is possible to perform first-principles MD of extended d-bonded systems, and opens a way to the study of complex materials, such as transition metal clusters and surfaces, amorphous transition metals, as well as all possible combinations with other elements.

Development of O(N) Methods

All electronic structure calculations to date, including Car-Parrinello simulations, have a numerical cost that asymptotically grows with size as N3, where N is the number of atoms. This is a consequence of the fact that the Kohn-Sham equations of density functional theory must be solved globally in order to determine the properties of any part of the cell. Recently, in collaboration with M. Parrinello of IBM Zurich Research Lab., we have suggested a new local description that can scale linearly with N [3]. Part of the calculations to demonstrate the validity of the approach have been performed on the NEC SX-3.

This scheme has been further improved leading to an algorithm which exhibits explicit linear scaling with N [4]. Numerical tests for both density functional and tight-binding Hamiltonians using a number of atoms up to few hundreds and few thousands, respectively, have been performed on the NEC SX-3. Combined with improved performances of computers, this new formulation will open the way to electronic structure calculations of unprecedented scale.

The performance of our codes on the NEC SX-3 is between 400 and 800 MFlops.

References

[1] Vittadini, A., A. Selloni, R. Car and M. Casarin. *Phys. Rev. B* 46 (1992): 4348.

[2] Pasquarello, A., K. Laasonen, R. Car, C-Y. Lee and D. Vanderbilt. *Phys. Rev. Lett.* 69(1992): 1982.

[3] Galli, G. and M. Parrinello. *Phys. Rev. Lett.* 69(1992): 3547.

[4] Mauri, F., G. Galli and R. Car. *Phys. Rev. B* (in press).

Computation of Unsteady Three-Dimensional Flows in Complex Geometries

L. Kaiktsis, K. Boulouchos and M.K. Eberle

I.C. Engines and Combustion Laboratory
ETH Zürich
Zürich, Switzerland

Most flows of practical interest are turbulent. The usual approach in computing turbulent flows is by averaging the governing Navier-Stokes equations over time and modeling the additional unknowns (Reynolds stresses) introduced by the averaging.

In this project we compute complex geometry flows in the late transitional - early turbulent regime, using direct numerical solution of the time-dependent Navier-Stokes equations. This approach, although computationally expensive, reveals all the details of the flow and can be very useful in assessing the validity of the various turbulence models.

Direct simulations require that all scales of turbulent motion be adequately resolved. This imposes severe requirements in terms of the required memory and CPU time, which increase dramatically with the flow's critical parameter, the Reynolds number. Therefore, direct simulations have been performed primarily for simple geometry flows at relatively low Reynolds numbers. The availability of supercomputers with performance in the Gigaflop range and main memory in the Gigabyte range makes the direct simulation of complex geometry flows feasible.

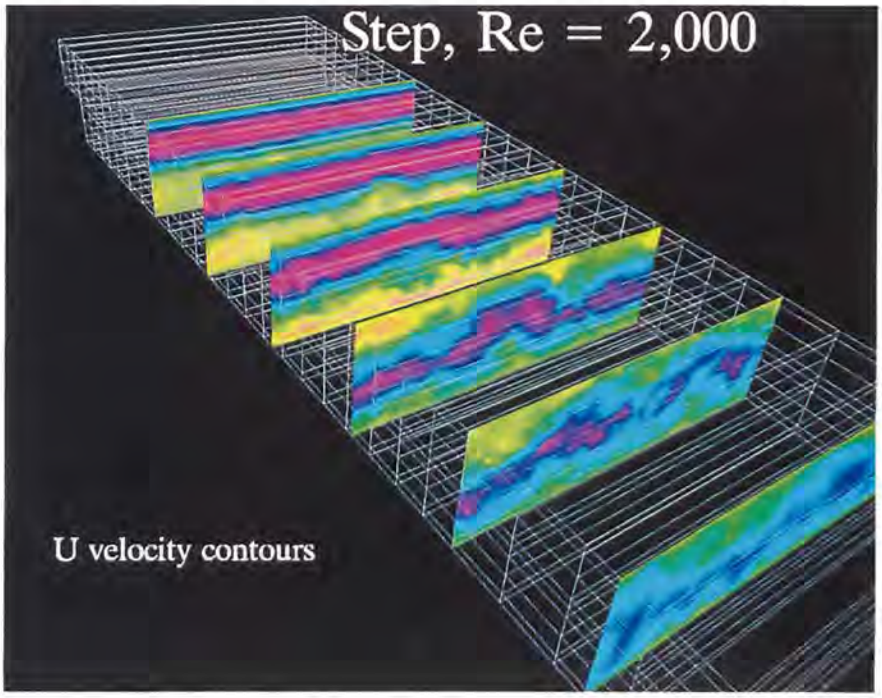

The numerical method used in our work is a Spectral-Element/Fourier method. For a nominally two-dimensional geome-

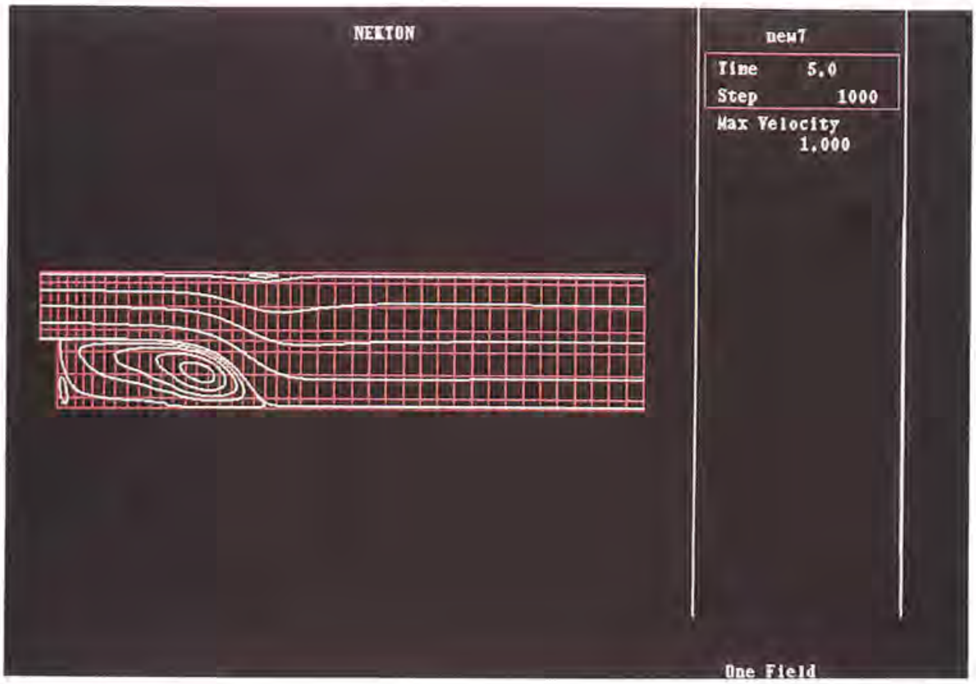

Figure 1. Streamline pattern of the equivalent two-dimensional velocity field at Reynolds number $Re = 2000$. The x and y scales are not the same; the computational domain extends to a total outflow length of 35 step heights.

try, Fourier expansions can be used to represent the field unknowns and data along the spanwise (homogeneous) z-direction. If the flow is Fourier analyzed in z, then the Navier-Stokes equations yield equations for the individual Fourier components. A fractional (splitting) step method in conjunction with a mixed explicit/implicit stiffly stable scheme is used for the time discretization. This results in two-dimensional Helmholtz equations for the pressure and the velocity components, for each Fourier component. The spatial discretization of those equations is performed using the spectral element methodology. In the standard spectral element discretization the computational domain is broken up into general quadrilaterals, which are mapped isoparametrically to canonical squares, within each, the geometry, the field unknowns and data are expressed as tensorial products in terms of Legendre-Lagrangian interpolants. Discrete equations are then obtained using Galerkin variational statements.

A direct simulation of the flow over a backward-facing step at Reynolds number is underway. This flow can be thought of consisting of three main components: the shear layer emanating from the step edge, the recirculation zone at the channel expansion, and the channel flow further downstream. Thus, it can serve as a prototype of a complex shear flow. After an equilibrium state is reached, the instantaneous fields are averaged and detailed turbulence statistics are calculated. Current results, based on averaging over 200 dimensionless time units illustrate interesting features of this flow. Figure 1 shows the streamline pattern of the equivalent two-dimensional field, obtained by averaging the instantaneous 3-D fields both in the homogeneous z-direction and in time. The computed value for the reattachment length is in very good agreement with experimental data, while the simulation illustrates the existence of a small corner eddy, also observed experimentally. The distribution of the Reynolds shear stress is plotted in Figure 2; higher values are obtained in the shear layer regions, and the global maxima are located upstream of the reattachment region. Finally, in Figure 3 the distribution of the skin friction coefficient, , along the low wall is presented. The region of negative values defines the primary recirculation zone, with being zero at the reattachment point.

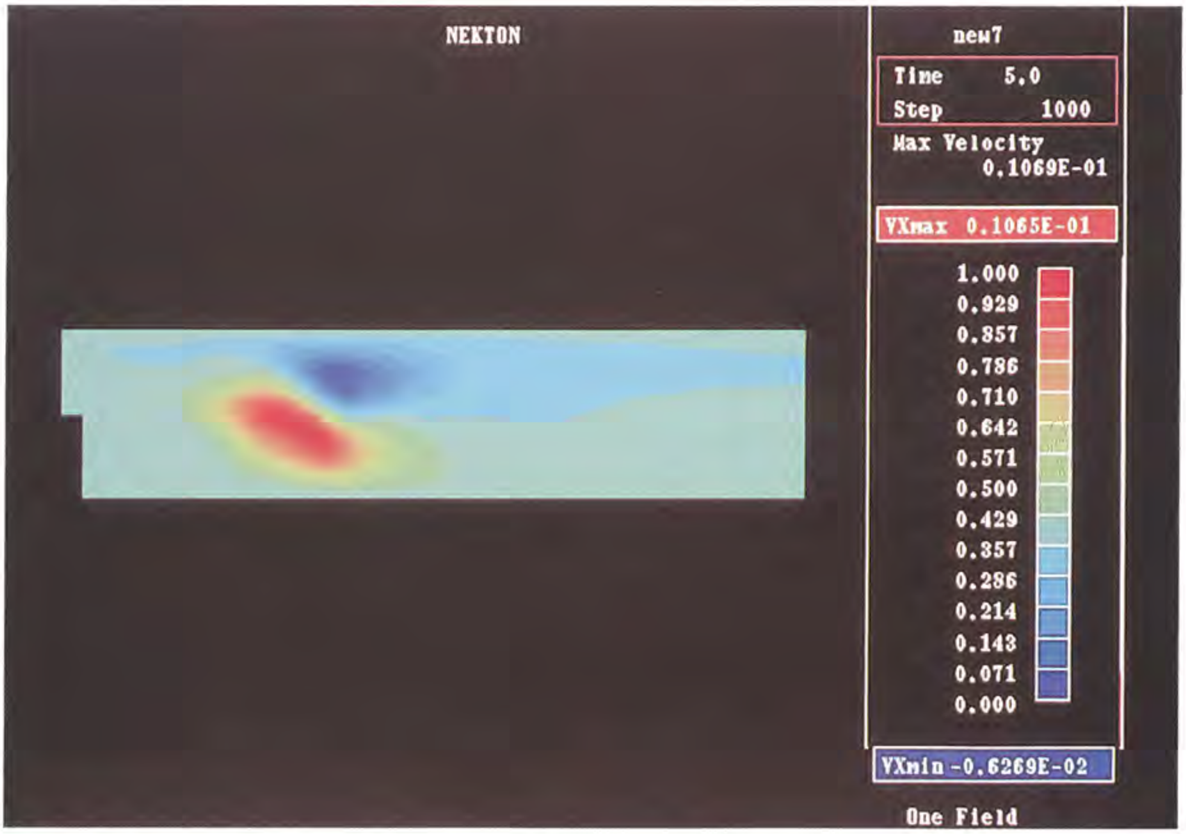

Figure 2. Colour-coded contours of the Reynolds shear stress $-\overline{U'V'}$, normalized by U^2_{max}, U_{max}, being the maximum velocity at the inflow. *Re* = 2,000.

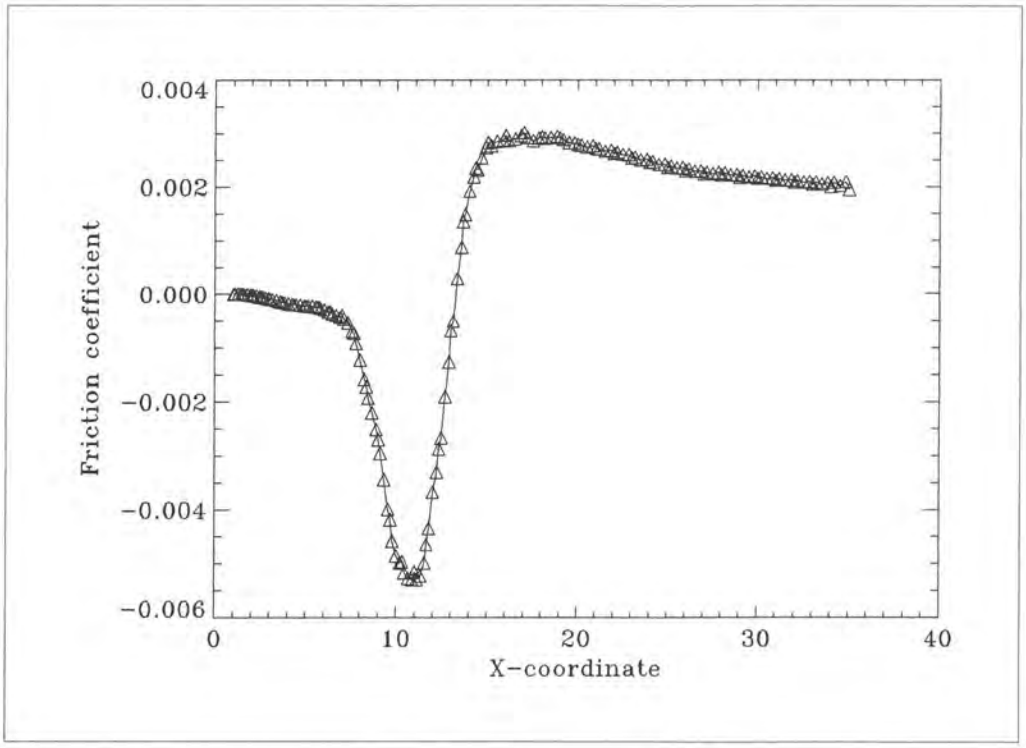

Figure 3. Low wall skin friction coefficient, defined as $C_f = \tau_w / (\frac{\rho}{2} U^2_{max})$, τ_w being the average wall shear stress, ρ the fluid density and U_{max} the maximum velocity at the inflow. *Re* = 2,000.

Environmental Sciences

Modeling of Global and Regional Climate Processes at CSCS

M. Beniston
Department of Geography
ETH Zürich
Zürich, Switzerland

The Scientific Issues

Global climate change has attracted much scientific and public attention in recent years, as a result of fears that man's economic activities are leading to an uncontrolled increase in Greenhouse Gas (GHG) concentrations, resulting in global rise in temperature due to the radiative properties of these gases. Predictions by atmospheric General Circulation Models (GCM) presented in the IPCC report (Intergovernmental Panel on Climate Change; Houghton et al., 1990) indicate that the lower atmosphere could warm on average by 1.5 - 4.5 C by the end of the next century. Among the possible consequences of this unprecedented rate of warming are increased desertification, sea-level rise, reduced water resources, collapse of intensive agriculture in the producing countries, irreversible ecosystem damage and loss of bio-diversity, and drop in energy availability. In the context of a rapidly increasing world population, global climate change will need to be prepared for by adaptation (which only the economically strong nations can afford) or prevention (which has not yet been accepted widely enough by political decision makers).

Figure 1 illustrates the major components of the climate system. Of central, but not single, importance is the atmosphere, which is probably the most rapidly reacting element of the climate system to internal and external forcing. The atmosphere is made up principally of three gases - oxygen, nitrogen, and argon - but also of minor quantities of other gases, such as carbon dioxyde (CO_2), methane (CH_4), nitrous oxide (N_2O), and totally artificial molecules such as the chloro-fluoro-carbons (CFC). Despite their very small concentrations - CO_2 represents about 300 parts per million by volume - their role in the thermal structure of the atmosphere is of prime importance. Indeed, in the absence of CO_2 or CH_4, the average temperature of the atmosphere would be 35 C less today, thus preventing any form of life on our planet. However, since the beginning of the industrial era, and the fact that the world population has increased quasi exponentially since that time, GHGs have increased at a very high rate compared to the natural fluctuations of these gases. It is the increase of GHGs, and the desequilibrium in the natural uptake or absorption of the trace gases, that lead climate specialists to believe that the atmosphere will undergo a period of accelerated warming.

A second major component of the climate system is the ocean, which acts as a regulator of atmospheric temperature and gas concentrations. The exchange of heat and moisture between the ocean and the atmosphere is a key process which is still incompletely understood. The complex surface and deep ocean circulation currents transport and store enormous quantities of heat and GHGs, and a more complete understanding of the climatic role of the ocean through modelling and observations is required. Recent results indicate that CO_2 uptake by the ocean is perhaps less important than previously estimated, so that probably a vital climate control is in the biosphere. Living organisms, particularly forests and plants, play a key role in atmospheric heat, moisture, and energy budgets close to the surface. However, knowledge of two-way interactions between the biosphere and the atmosphere are too poorly known for their effects to be adequately included in present-day climate models. A detailed program on the climatic influence of the biosphere needs to be urgently initiated, in order to incorporate in a statistically meaningful manner the biospheric element in a climate model. Other components of the climate system include the cryosphere - continental ice caps and floating sea ice - whose mechanisms include instabilities in the general circulation of the atmosphere resulting from temperature differences between the Poles and the Equator. In addition, the surface energy balance is significantly influenced by the high reflectivity, or albedo, of the ice. The seasonal fluctuations of sea ice, and its possible disappearance in the Arctic Ocean in a warmer atmosphere, could have significant repercussions on accelerated global warming.

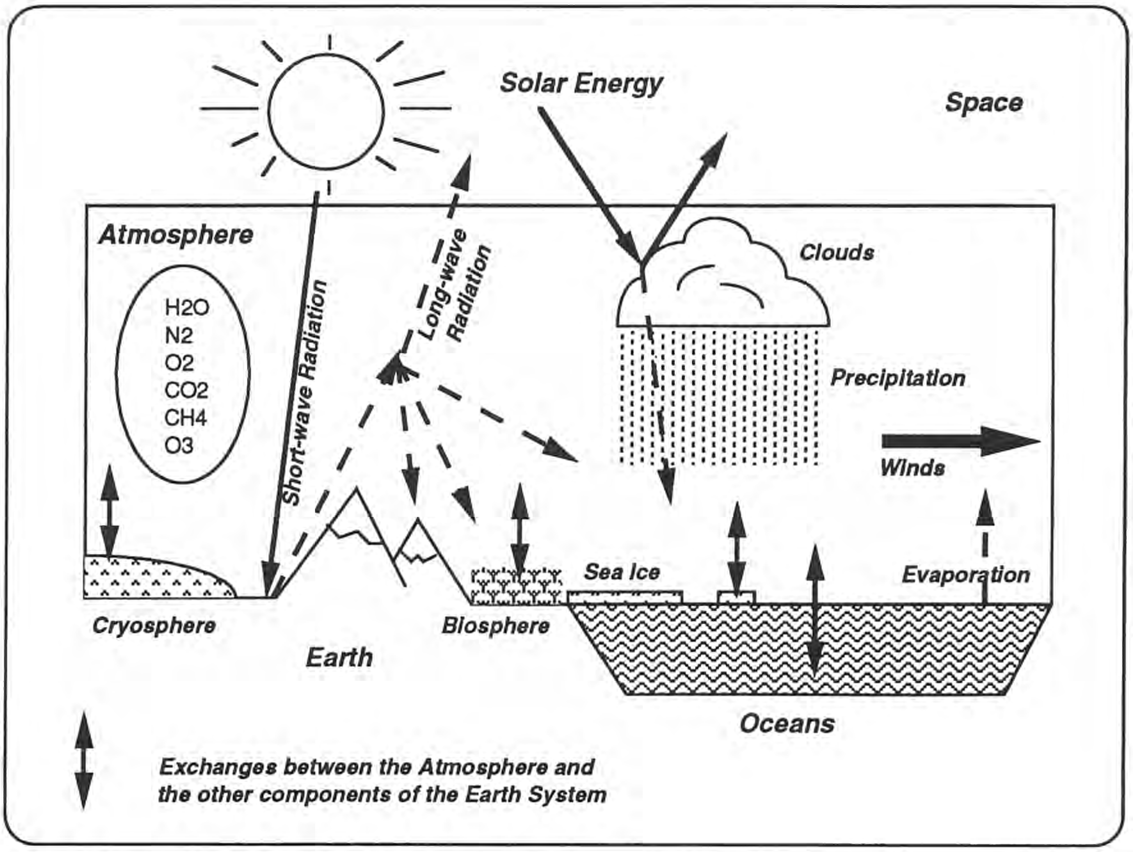

Figure 1: Schematic illustration of the climate system

A major problem in attempting to model the climate system as a whole is linked to the vastly different time scales characteristic of the individual components of the system described above. As seen in Figure 2, the oceanic, biospheric, and cryospheric processes have vastly different response times than the atmosphere to a particular forcing, so that coupled model approaches in order to investigate interactions and feedback between elements of the system are by no means trivial.

General Circulation Models (GCM) are those which attempt to incorporate as many elements of the above described systems as possible. They are amongst the largest and most demanding operational applications in terms of computing resources. They typically solve large sets of equations at up to several hundred thousand grid-points, and these computations must be repeated 50 or more times per simulated day in order to represent the temporal evolution of the system with enough accuracy. Because the GCMs are producing results over a network of grid points distributed in three-dimensions over the globe, computer time and space requirements are extremely large, and

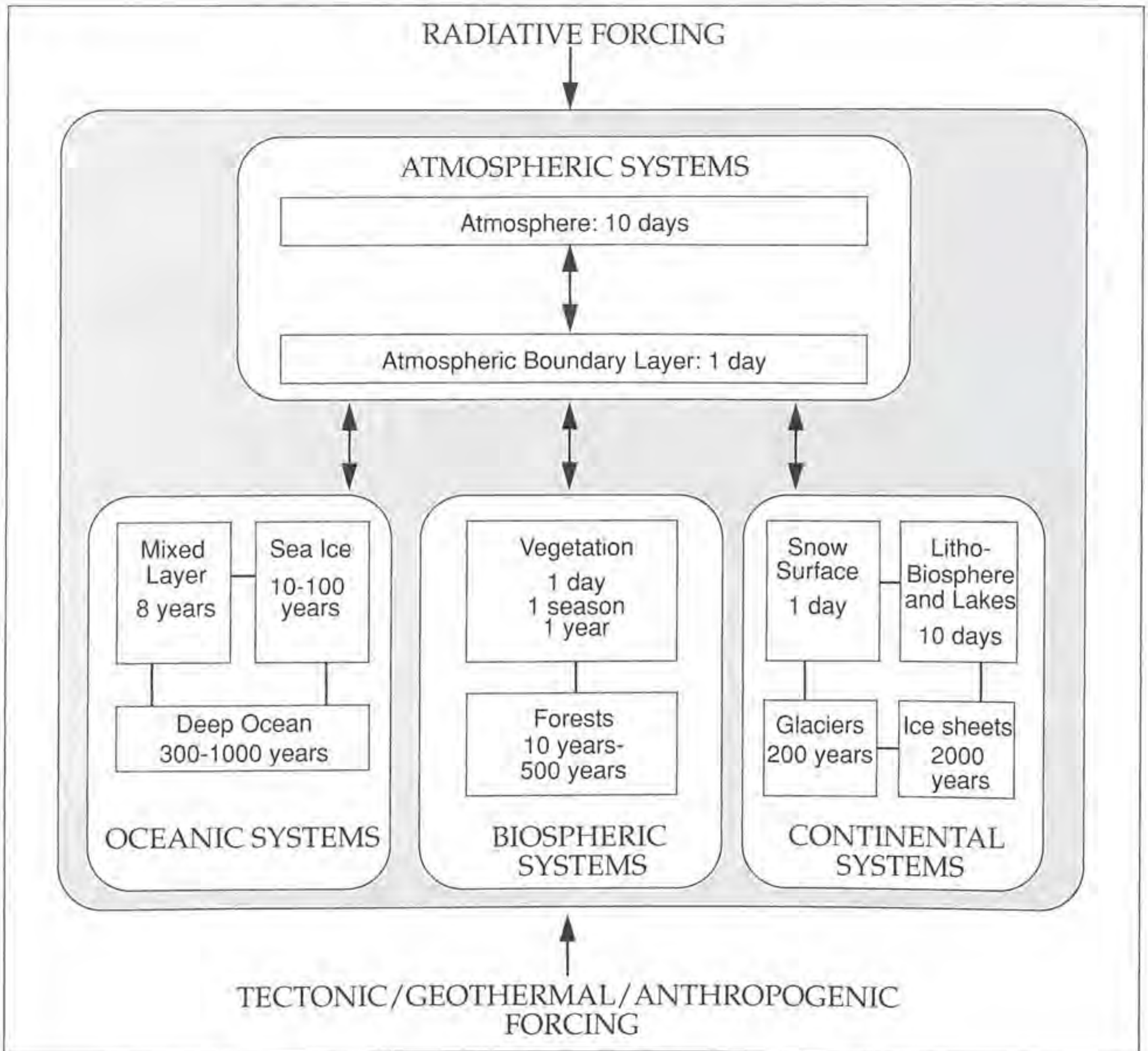

Figure 2: Characteristic time scales of various components of the climate system

much of the physics representing feedback within the climate system needs to be parameterized, often in an oversimplified manner. As already mentioned above, the coupling of such systems within a single modelling system is still in its infancy and is by no means a trivial matter. As an example of computing resource requirements, an advanced model such as the Max-Planck-Institute T-106 spectral model (wave number truncation 106, corresponding to a spatial resolution of approximately 120 km over the globe) requires 270 hours of CRAY-2 time to simulate a one-year atmospheric cycle. The data generated for this one-year period is about 16 Gbytes (Bengtsson, 1991, personal communication).

Despite the impressive computational resources used for climate modelling, GCMs have a far too low resolution to provide any meaningful data on the regional scale; the "regional" experiments undertaken during the IPCC process (Houghton et al, 1990) were disappointing at best. This type of data is, however, essential for impact modellers and political decision makers. Waiting for high-resolution GCM climate simulations in coming years as new generations of supercomputers come onto the market is probably not an optimal solution. Whereas higher resolution has led to marked improvements in forecasting skills for 5-10 days, a corresponding improvement for *climatological-scale* problems cannot be expected, because in the climate system scale is not the only dominant feature of the problem to be solved. The feedback from other components of climate, in particular the oceans, the cryosphere, and the biosphere, will also play a determining role in the evolution of climate forced by increased GHG concentrations. Despite improvements in recent years in the coupling of different systems to atmospheric GCMs, there are still many uncertainties and unknowns in the simulation of coupled systems. In addition, climate is an inherently chaotic system, so that a measure of unpredictability will always need to be kept in mind when analysing GCM climate statics, whatever the resolution of the climate model. Regional climate predictions cannot be solved solely by increased computer power and high resolution models. They will progress through a better integration of ocean, ice and biological processes and feedback mechanisms with the atmosphere. This implies major investments in interdisciplinary research, which in turn requires breaking through the traditional barriers of the different disciplines, in order to achieve a convergent approach to research in climate and global change.

Climate Modelling in Switzerland

As a result of joint research agreements with international climate modelling groups, new initiatives in climate relevant research have been made possible; climate modelling is now beginning in collaboration with the Max-Planck-Institute for Meteorology in Hamburg, who have installed in 1992 the high-resolution atmospheric General Circulation Model (GCM) at CSCS. The Hamburg GCM is now beginning to produce first results--indeed for the first time anywhere in the world, a climate model is operating at such a detailed spatial scale, and these will be of use to the two major project funded by the Swiss National Science Foundation relating to climate.

Additional work has been done in 1992 in the field of regional modelling, as a preparation for the coupling of mesoscale and global models to improve the definition of climatological variables over regions of specific interest. The case studies for which the DREAMS (Differential equation REgional Atmospheric Modelling System) model has been used is for the regions of Athens, in the context of an international atmospheric model intercomparison study.

The two preliminary research orientations for which global and regional models will be used in Switzerland with the resources of CSCS are the following;

Numerical Simulations of Climate Scenarios in the Alps

The objective of the project, funded by the NFP-31 program on Climate Change and Natural Hazards is to gain experience in the handling and use of a General Circulation climate mode; to nest a

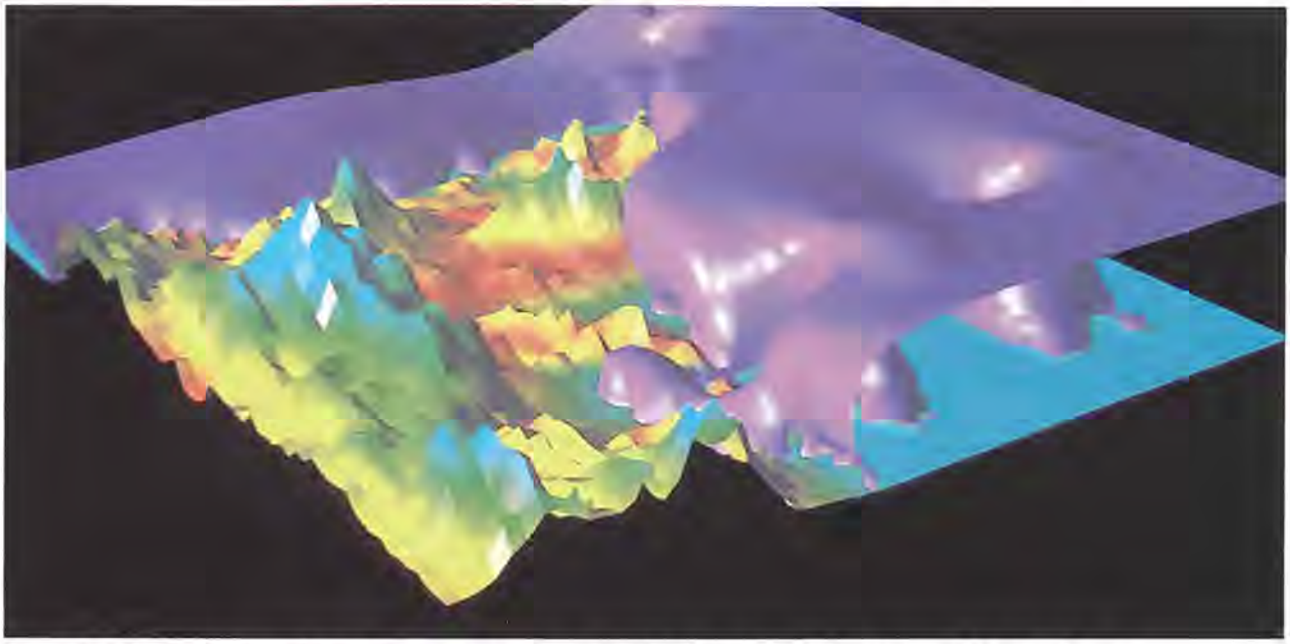

Figure 3: 3-D visualization of the pressure structure over land and sea area in the region of Athens, Greece.

high-resolution mesoscale model to obtain reasonable regional predictions of climate and water regimes. Such models will be used to evaluate modification in atmospheric flows over WEstern Europe and in particular over the Alpine region under different boundary conditions, in particular experiments with transient doubling of carbon dioxide concentrations globally.

Transient simulations are necessary to provide a more realistic approach to future evaluation of climate than the equilibrium (i.e., instantaneous) response to increases in greenhouse gas concentrations. Model simulations should ideally begin in the decade 1981 - 1990 for which an enormous amount of observational data is available for initialization and intercomparisons. The simulations should be pursued over a fifty-year period, i.e. through to the decade 2041-2050.

The model statistics will be thoroughly investigated to determine significant shifts in climate trends over the Alps. The analyses will provide quantitative estimates of the future statistical structure of climate over Switzerland; it will then be possible to reconstruct a typical yearly climatology based on existing data for meteorological episodes which have prevailed in the recent past. In this manner, significant progress can be made on climate scenarios for use in the assessment of climate change impacts on the natural and the socio-economic environments.

During the proposed period, a priority is set for simulating the near-surface features of climate, especially the energy and water balance. Another equally-important aim is to start to develop expertise by young scientists in the handling of complex climate models.

Influence of the Alps on Continental-scale Climate

The Alps are a significant barrier to flow dynamics, leading to effects such as lateral wind deflection resulting in regional wind systems, orographically-induced turbulence, wave breaking, and vertical shear forced by the flow deflection. Atmospheric heating is also affected by topography, and meso- and synoptic-scale investigations by different groups have in recent years underlined the significance of the thermal effect of mountains, via vertical turbulent transfers not only of momentum, but also of latent and sensible heat. The research proposed in this study will be to identify the weaknesses of General Circulation Climate Models (GCMs) at various resolutions in the representation of these phenomena, to investigate in more detail the nature of turbulent transfers of heat, moisture, and momentum in the presence of orography using real atmospheric data, any available remote-sensing data, and results from mesoscale atmospheric models being operated by other partners within the Module 1 of the Priority Program on Environment (SPP-Umwelt). The findings of these investigations will be synthesized in the form of suggestions for improved orographic parameterization techniques in GCMs.

Partners in these two projects, in addition to the initiators at the Department of Geography of ETH-Zürich (Prof. A. Ohmura, Dr. M. Beniston, Ms. R. Marinucci, Mr. P. Tschuck, and Mr. M. Wild) are the Max-Planck-Institute for Meteorology, Hamburg (Prof. L. Bengtsson, Prof. K. Hasselmann, Dr. U. Schlese), and the Joint Research Center of the EEC in Ispra (Prof. M. M. Verstraete, Dr. F. Giorgi, Dr. P. Martin). Other groups who have expressed interest include the Laboratoire de Méteorologie Dynamique, Paris (Prof. R. Sadourny, Dr. R. Butel), who carried out some preliminary benchmarking tests on the CSCS supercomputer in May, 1992, and the National Center for Atmospheric Research, Boulder, Colorado. As the climate modeling activities grow in Switzerland, then so will the extent of the international collaborations.

Publications

[1] Beniston, M. and J. Perez-Sanchez. "An Example of Climate-relevant Processes unresolved by Present-day General Circulations Models." *Env. Conserv.* 18 (1992): 165-169.

[2] Beniston, M. "Potential Environmental and Economic Impacts of Abrupt Colimate Change." *Proceedings, South Pacific Region Environment Programme (SPREP) Conference*, Nouméa, New Caledonia. April 1992.

[3] Beniston, M. "Prévisions climatiques pour les Alpes: une revue des techniques de régionalisation." *La Météorologie* 1992 (in press).

[4] Beniston, M. A review of the book entitled *Greenhouse Earth* by Annika Nillson. WMO Bulletin (1993, in press).

[5] Beniston, M. "Overview and Synthesis of the International Conference on Mountain Environments in Changing Climates." *Bull. Amer. Meteol. Soc.* (1993, accepted)

[6] Ehinger, J. and M. Beniston. "APSIS Model Intercomparison Experiment. Part A: First Results of Atmospheric Dynamics Over the Region of Athens With the DREAMS Numerical Modeling System." *Env. Software* (1993, accepted).

Personnel

CSCS Staff

Management

Decker, Karsten
Director of Research and Development

Gruber, Ralf
Director of Scientific Applications

Pelloni, Norman
Director of Technical Operations

Scheidegger, Alfred
Director of CSCS

Technical Operations

Anastasi, Andreas
Technical infrastructure and CMCM

Gay, Mario
System managment

Giordano, Silvia
Network managment

Mari, Gianpaolo
Technical infrastructure

Mastropietro, Roberto
System managment and CMCM

Thibaud, Jean-Louis
System managment and CMCM

Scientific Applications

Ballabio, Mauro
Application software

Barker, David
Application software (NEC)

Bernasconi, Andrea
Application software

Chiu, Jia Yu
Application software (NEC)

Hodous, Michael
Application software and CMCM

Mangili, Angelo
Graphic software

Maric, Djordje
Application software

Meyer, Urs
Visualization and CMCM

Stoll, Erich
Application software (University of Zürich)

Tomassini, Marco
Application software and CMCM

Research and Development

Dvorak, Jiri
Software R&D

Rehmann, René
Software R&D

Rühl, Roland
Software R&D

Central Functions

Buzzini, Ines
Secretariate

Londino, Letizia
Secretariate

Nart, Carla
Secretariate and personnel administration

Schaidl Meyer, Elena
Library

Vecchi, Nicole
Publications

Zumthor, Bernardo
External and user relations

NEC Site Support

Hirano, Kinya
Hardware maintenance

Ishii, Masahiko
System maintenance/ support

Takagi, Yasushi
Hardware maintenance

CSCS Functional Architecture

The functional architecture of CSCS was introduced in mid-1992 and is based on a central management core from which function lobes radiate. This structure fosters an integrative management style, encourages inter-sectional project development, and functional expansion can easily be accommodated by the addition of a new lobe.

Central management is surrounded by common management committee members (CMCM) who are representatives of the function lobes.

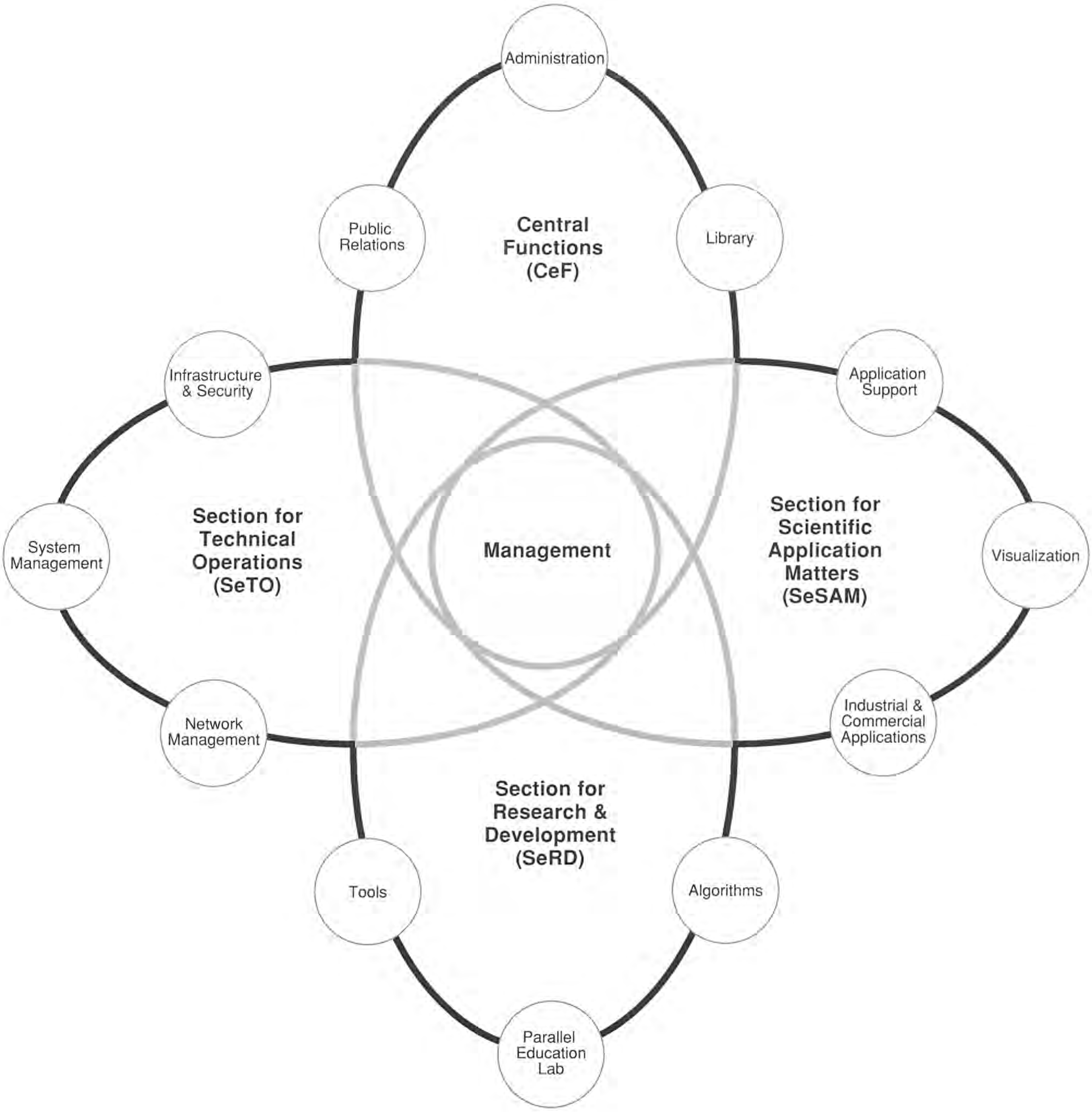

Visitors

Banfi, F.
University of Neuchatel, Switzerland
Student: stage period
(July -August 1992)

Beniston, Dr. M.
Geograpisches Institut, ETH Zürich, Switzerland
Installation on the SX-3 of a meso scale finite difference grid-point model for mid-latitude convection and scale interaction studies
(Several visits)

Butel, Dr. R.
Laboratoire de Meteorologie Dynamique, Paris, France
Preparation of the installation of the LMD climate model using several polynomial benchmarks
(June 1992)

Cotting, R.
University of Zürich, Switzerland
Visualizing the quantum dynamics of a radiationless decay of nitrosyl fluoride (FNO) after laser excitation of the first UV absorption band
(June 1992)

Flükiger, Dr. P. F.
University of Geneva, Switzerland
Postdoc stage: adaptation of a Molecular Graphics Package to the CSCS Graphics Laboratory equipment and extensions to the original software
(from November 1992)

Graziani, Dr. G. and Dr. P. **Thunis**
Joint Research Center of the Commission of the European Community, Ispra, Italy
Installation on the SX-3 of a numerical tool to help in environmental assessments and evaluations
(October 1992)

Hakkarinen, Dr. C.
Electric Power Research Institute, Palo Alto, U. S. A.
Discussion on possible collaboration between CSCS and Model Evaluation Consortium for Climate Assessment (MECCA)
(December 1992)

Kaiser, B.
University of Zürich, Switzerland
Student: design and implementation of an object-oriented ray-tracing environment with C++
(February 1992)

Kratky, Dr. M. and Dr. J.**Rogalewicz**
Institute of Physics, Czechoslovak Academy of Sciences, Praha, Czechoslovakia
Studies on running a supercomputer center, user support and programming a graphics interface
(January - February 1992)

Macrae, Dr. R. M.
Rutherford Appleton Laboratory, Hartwell UK
Density functional calculations for muonium sites in elemental semiconductors
(October-November 1992)

Medvedev, Dr. S.
Keldysh Insitute for Applied Mathematics, Moscow, CUI
Development of equilibrium and stability programs for Doublet geometries. "MHD Equilibrium Code for Asymmetric Plasma with Separation" with L. Villard, R. Gruber and S. Merazzi (Technical report CSCS-TR-93-01)
(June 1992 - February 1993)

Nadrchal, Prof. J. and Dr. V. **Kriz**
Institute of Physics, Czechoslovak Academy of Sciences, Praha, Czechoslovakia
Studies on the usage of supercomputers in Switzerland and data compression
(April 1992; November 1992)

Paschedag, N.
University of Zürich, Switzerland
Calculation and visualization of spin density scalar fields of carbon and silicon clusters containing impurities
(June 1992)

Pfistner, C.
University of Bern, Switzerland
"Thermal Beam Distortions on Longitudinal Pumped Solis State Lasers" with R. Weber, H. P. Weber, S. Merazzi and R.Gruber (Technical Report CSCS-TR-93-02)
(Several visits)

Pontiggia, I.
University of Neuchatel, Switzerland
Diploma thesis: color correction for a color laser copier and implementation of a testbed
(from November 1992)

Schlese, Dr. U.
Max-Plank-Institut für Meteorologie, Hamburg, Germany
Installation on the SX-3 of the ECHAM program for climate simulation
(April 1992)

Widmann, A.
ETH Zürich, Switzerland
Monte-Carlo simulation of polymethylene
(December 1992)

Wild, M., P. **Tschuck** and S. **Kaelin**
ETH Zürich, Switzerland
Global and regional (alpine) climate simulation with high-resolution models
(Several visits)

Wilson, Dr. J.
Joint Research Center of the Commission of the European Community, Ispra, Italy
Preparation for porting of the MANGUNTIA global climate model to the SX-3
(September 1992)

Publication Review

CSCS Member Publications

(CSCS members are indicated with bold type.)

Bernasconi, A. (*see* Cox, P. T.)

Bonomi, E. and **M. Tomassini.** "Massively Data-Parallel Molecular Dynamics." *International Journal of Modern Physics C* 3(1992): 709-731.

_____. "Data-Parallel Simulation of Hard-Particle Systems." *Computer Physics Communications* 73(1992): 40-46.

_____. "The Role of Massively Data-Parallel Computers in Large-Scale Molecular Dynamics Simulations." In *Proceedings, 4th International Conference on Computational Physics,* Prague, Czechoslovakia. 1992.

Brieger, L., E. Bonomi and **M. Tomassini.** "Lattice Gas Model of a Parallel Flow." In *Proceedings, Workshop on Cellular Automata Models for Astrophysical Phenomena,* Liege, France. 1992.

Chopard, B. and **M. Tomassini.** "High-Speed Cellular Automata Simulations of Reaction-Diffusion Processes on the NEC SX-3." *EPFL Supercomputing Review* 4 (1992): 9-12.

Claxton, T.A., **D. Maric**, and P. F. Meier. "Dynamic Model for the Structure of Bond-Centered Muonium in Silicon." *Physical Review B* (in print).

Cooper, W.A., S. P. Hirshman, **R. Gruber** and **S. Merazzi**. "3-D Magnetohydrodynamic Equilibria with Anisotropic Pressure." *Computer Physics Communications* 72 (1992): 1-13.

Cooper, W.A., Y. Nakamura, M. Wakatani, **R. Gruber, S. Merazzi**, D. V. Anderson and U. Schwenn. "Linear MHD Stability Computations in 3-D Plasmas." In *Proceedings, International Conference on Plasma Physics,* Innsbruck, Austria. 1992.

Cox, P.T., G. Sozzi, G. Ballocchi, **A. Bernasconi**, R. E. Breedon, L. Camilleri, R. L. Cool, P. Cushman, L. Dick, E.C. Dukes, B., Gavioud, G. Gaille, P. Giacomelli, D. Hubbard, J. B. Jeanneret, C. Joseph, W. Kubischta, J. F. Loude, E. Malamud, C. Morel, P. Oberson, O. E. Overseth, J. L. Pagès, J. P. Perroud, D. Rüegger, R. W. Rusack, V. Sing, G. R. Snow, D. Steiner, L. Studer, M. T. Tran, A. Vacchi, G. Balenti and M. Werlen. "Direct Photon Production in Antiproton-Proton and Proton-proton Interactions at $\sqrt{s} = 24.3$ GeV." *Physics Letters B* (submitted 1992; CERN-Lausanne-Michigan-Rockefeller collaboration).

Decker, K. and R. M. Rehman. " ADE--An Application Development Environment for Transparent Use of Scalable Parallel Architectures." In *Proceedings, IFIP WG 10.3 Working Conference on Programming Environments for Parallel Computers,* Edinburgh, England, edited by N. P. Topham, R. N. Ibbett and T. Bemmerl. April 6- 8, 1992. Amsterdam: Elsevier Science Publishers B.V., 1992.

_____. "Simple and Efficient Programming of Parallel Distributed Systems for Computational Scientists." Technical Report IAM-92-019, University of Berne, Switzerland, October 1992.

Estreicher, S. K. and **D. Maric**. "What is so Strange about Hydrogen Interactions in Germanium?" *Physical Review B* (submitted 1992).

Fu, G. Y., W. A. Cooper, U. Schwenn, **R. Gruber, S. Merazzi** and D. V. Anderson. "Full 3-D Ideal MHD Stability Analysis of Low-n Modes and Mercier Modes in Stellerators." *Physics of Fluids* (accepted for publication 1992).

Gruber, R. "The Swiss Scientific Computing Centre." In *Proceedings, CATSUPERCOMP,* Barcelona, Spain. 1992.

_____. "Anisotropic Pressure Numerical 3D MHD Equilibria." In *Proceedings, International Conference on Plasma Physics,* Innsbruck, Austria. 1992.

Gruber, R. and **M. Hodous**. "Optimization on the NEC SX-3." *Speedup Journal* 6(1)(1992): 38-40.

Gruber, R. (*see also* Cooper, W. A.; Fu, G. Y.; Pfistner, C.)

Hodous, M. (*see* Gruber, R.)

Maric, D., P. F. Meier and S. K. Estreicher. "{H,B}, {H,C} and {H,Si} Pairs in Silicon and Germanium." *Physical Review B* (in print).

Maric, D. (*see also* Claxton, T.A.; Estreicher, S. K.; Paschedag, N.)

Merazzi, S. "B2000 System Manuals-Graphical Tools Reference Manual." SMR Corporation, Bienne, Switzerland (1992).

Merazzi, S. (*see also* Cooper, W. A.; Fu, G. Y.; Gruber, R.; Pfistner, C. p. 60)

Meyer, U. "Das Geoid - Methoden der Computergrafik zur dreidimensionalen Visualisierung." In *Vermessung Photogrammetrie Kulturtechnik* 7 (July 1992): 405-406.

Paschedag, N., H. U. Suter, **D. Maric** and P. F. Meier. "Configuration Interaction Calculation of Hyperfine Properties for Bond-centered Muonium in Diamond." *Physical Review Letters* (in print).

Rehmann, R. M. " An Application and Program Development Enviroment for Multiprocessor Systems with Distributed Memory." Ph.D. Thesis, IAM, University of Berne, Switzerland, July 1992.

_____. "A Macro Communication Package for Master-Slave Models on DMPPs." Technical Report IAM-92-020, University of Berne, Switzerland, October 1992.

Rehmann, R. M. (*see also* Decker, K.)

Scheidegger, A. "Anforderungs Profil des Ingenieurs: Wettbewerbsfaktor Informations- und Kommunikationstechnologie." *Schweizerische Arbeitgeber-Zeitung.* 44(1992): 1208-1210.

_____. "Un atout indispensable à la compétitivité de l'ingénieur" *Journal des Associations patronales* 44 (1992): 1219-1221.

Tomassini, M. (*see* Bonomi, E.; Brieger, L.; Chopard, B.)

CSCS Visitor Publications

(CSCS visitors are indicated with bold type.)

Elfimov, A. G., **S. Yu. Medvedev** and G. A. Pestryakova. "Fast Wave Spectral Properties in ITER Tokamak." In *Proceedings, 19th EPS Conference Controlled Fusion and Plasma Physics,* Innsbruck, Austria. 1992.

Flükiger, P. "Development of the Molecular Graphics Package MOLEKEL and its Application to Selected Problems in Organic and Organometallic Chemistry." Ph. D. thesis 2561, University of Geneva, Switzerland, December 1992.

Flükiger, P., J. Weber, R. Chiarelli, A. Rassat and Y. Ellinger. "Chirality and Spin Density: Ab-initio and Density Functional Approaches." *International Journal of Quantum Chemistry* (accepted for publication).

Flükiger, P. (see also Weber, J.; Morgantini, P. Y.; Furlan, A.)

Furlan, A., T. Fischer, **P. Flükiger**, H.-U. Gudel, S. Leutwyler, H. P. Lüthi, M. J. Riley and J. Weber. "The Low-Frequency Vibrations of Triptycene." *J. Phys. Chem.* 96 (1992): .10713-10719.

Medvedev, S. Yu. and S. E. Sharapov. "Stabilizing Effect of Trapped Alpha Particles on Low-frequency MHD Ballooning Modes in ITER Plasmas with Flat Q Profiles." *Fusion Technology* 22 (1992): 470-473.

Medvedev, S. Yu. (*see also* Elfimov, A. G.).

Morgantini, P. Y., **P. Flükiger** and J. Weber. "Computer Modeling of the Activation Processes of the Aromatic Nucleophilic Substitution Mechanism." *Journal of Chemical Physics* 89 (1992): 1723.

Pfistner, C., R. Weber, H.P. Weber, S. Merazzi and R. Gruber. "Thermal Beam Distortions in Longitudinally Pumped Solid State Lasers." *IEEE Journal of Quantum Electronics* (to be published).

J. Weber, D. Stussi, **P. Flükiger** and P. Y. Morgantini. "Development and Applications of an Extended-Huckel-based Reactivity Index for Organometallic Complexes." *Comments Inorganic Chemistry* (accepted for publication).

CSCS User Publications

(based on computations performed using CSCS computer facilities)

Alexandrou, C. *Speedup Journal* 6(1) (1992): 41.

Alexandrou, C., S. Güsken, F. Jegerlehner, K. Schilling and R. Sommer. Paul Scherrer Institute report PSI-PR-92-27; PSI-PR-28. (to appear in "Lattice '92" *Nuclear Physics*, proceedings supplement).

_____. *Phys. Lett. B* 256(1991): 60; *Nuclear Physics B* 374 (1992): 263.

Alexandrou, C. (*see also* Sommer, R.)

Ancilotto, F. *Physics Review* 43 (1991): 5180.

Ancilotto, F. and A. Selloni. *Physical Review Letters* 68 (1992): 2640.

Ancilotto, F., A. Selloni and E. Tosatti. *Physics Review* 43 (1991): 14726.

Ancilotto, F., W. Andreoni, A. Selloni, R. Car and M. Parrinello. *Physical Review Letters* 65 (1990): 3148.

Ancilotto, F. (*see also* Selloni, A.)

Assaad, F.F. and D. Würtz. *Physics Review B* 44 (1991): 2681.

Beniston, M. "Potential Environmental and Economic Impacts of Abrupt Colimate Change." *Proceedings, South Pacific Region Environment Programme (SPREP) Conference*, Nouméa, New Caledonia. April 1992.

_____. "Prévisions climatiques pour les Alpes: une revue des techniques de régionalisation." *La Météorologie* 1992 (in press).

Beniston, M. and J. Perez-Sanchez. "An Example of Climate-relevant Processes unresolved by Present-day General Circulations Models." *Env. Conserv.* 18 (1992): 165-169.

Blandin, P., C. Massobrio and J. Buttet. "Dynamics of Silver Dimer Deposition on Platinum Surfaces." In *Proceedings, Materials Research Society Symposium* Vol. 278 (1992).

_____. "Equilibrium properties of Ag clusters on Pt (111)." In *Proceedings, ISSPIC '92.* (also to be published in *Zeitschrift für Physik D*).

Blandin, P. and C. Massobrio. "Diffusion properties and collisional dynamics of Ag adatoms and dimers on Pt (111). " (to be published in *Surface Science Letters*, December 1992).

Car, R. and M. Parrinello. *Physical Review Letters.* 55 (1985): 2741.

Continenza, A. and P. Monachesi. "Electronic Properties of Isostructural Intermetallics of Ce." *Journal Magnetic Materials* 1308 (1992): 104-107.

_____. "Volume Effects on the Magnetic Properties of Cubic Isostructural Intermetallics of Ce." *Physics Review B* 46 (1992): 6217.

Continenza, A. (*see also* Monachesi, P.)

de Pablo, J. J., M. Laso, and U. W. Suter. *Journal of Chemical Physics* 96(3) (1992): 2395.

_____. *Journal of Chemical Physics* 96(8) (1992): 6157.

_____. *Siepmann Molecular Physics* (in press, 1992).

de Pablo, J. J. (*see also* Laso, M.)

Engel, P. "The Enumeration of Four-dimensional Polytopes." *Discrete Math.* 91 (1991): 9-31.

Eggenberger, R. and H. Huber. "Comparison of the Performance of a Program for Molecular Dynamics of Liquids on Different Computers." *CHIMIA* 46 (1992): 227.

Eggenberger, R., S. Gerber, H. Huber, D. Searles and M. Welker. "*Ab initio* Calculation of the Shear Viscosity of Neon in the Liquid and Hypercritical State Over a Wide Pressure and Temperature Range." *Chemical Physics* 164 (1992): 321.

_____. "*Ab initio* Calculation of the Thermal Conductivity of Neon in the Liquid and Hypercritical State Over a Wide Pressure Range." *Molecular Physics* 76 (1992): 1213.

_____. "*Ab initio* Calculation of the Deuterium Quadrupole Coupling in Liquid Water." *Journal of Chemical Physics* 97 (1992): 5898.

Galli, G. and M. Parrinello. *Physical Review Letters* 69 (1992): 3547.

Guentert, P., V. Dötsch, G. Wider and K. Wüthrich. *Journal of Biomolecular NMR* (in press, 1992).

Grünbaum, B. and V. P. Sreedharan. "An Enumeration of Simplicial 4-polytopes with 8 Vertices." *Journal of Combinatorial Theory* 2 (1967): 437-465.

Kleinschmidt, P. "Sphren mit wenigen Ecken." *Geom. Dedicata* 5 (1976): 307-320.

Laso, M., J. J. de Pablo and U. W. Suter. *Journal of Chemical Physics* 97(4) (1992): 2817.

Laso, M. (see also de Pablo, J. J.)

Lerch, P., T. Jarlborg and E. G. Moroni. *Proceedings, ICPTM 1992*, Darmstadt. (in press).

Lerch, P., E. G. Moroni and T. Jarlborg. (to be submitted to *Physics Review B*).

Lüthi, H-P. (see Furlan, A.)

Mani, P. "Spheres with Few Vertices." *Journal of Combinatorial Theory* A13 (1972): 346-352.

Monachesi, P. and A. Continenza. "Effect of Composition on the Anderson Hybridisation in Ternary Cubic Alloys of Ce." *Nuovo Cimento D* (in press).

Monachesi, P., L. C. Andreani, A. Continenza and A. K. McMahan. "Volume Dependence of Anderson Hybridisation in Cubic CeAg and CeCd." *Journal of Applied Physics* (in press).

Monachesi, P. (*see also* Continenza, A.)

Nishino, T. and K. Ueda. "Spin and Charge Excitation Gaps in One-Dimensional Periodic Anderson Model." (preprint).

Ogata, M., M.U. Luchini, S. Sorella and F.F. Assaad. *Physical Review Letters* 66 (1991): 2388.

Parrinello, M. (*see also* Car, R.; Galli, G.)

Pasquarello, A., K. Laasonen, R. Car, C-Y. Lee and D. Vanderbilt. *Physical Review Letters.* 69 (1992): 1982.

Podloucky, R., S. G. Steinemann and A. J. Freeman. In *Proceedings, Material Research Society Symposium* 252 (1992): 43.

_____. *New Journal of Chemistry* (in press, 1992)

Quack, M. and M. A. Suhm. "Potential Energy Surfaces, Quasiadiabatic Channels, Rovibrational Spectra, and Intramolecular Dynamics of (HF)_2 and its Isotopomers from Quantum Monte Carlo Calculations." *Journal of Chemical Physics* 95 (1991): 28-59.

Quack, M., J. Stohner and M. A. Suhm. "Vibrational Dynamics of (HF)_n Aggregates from an *ab initio* Based Analytical (1+2+3)-body Potential." *Journal of Molecular Structure* (in press, 1993).

Selloni, A., F. Ancilotto, N. Takeuchi and A. Vittadini. In *Proceedings, 21st International Conference on the Physics of Semiconductors*, Beijing, China. August 1992 (in press).

Selloni, A. (*see also* Vittadini, A.; Takeuchi, N.)

Sommer, R., C. Alexandrou, S. Güsken, F. Jegerlehner and K. Schilling. *Nuclear Physics B* (Proc. Suppl.) 20 (1991): 493; *Nuclear Physics B* (Proceedings Supplement) 26 (1992): 387.

Sommer, R. (*see also* Alexandrou, C.)

Suhm, M. A., J. T. Farrell, Jr., S. Ashworth and D. J. Nesbitt. Manuscript in preparation.

Suhm, M. (*see also* Quack, M.)

Takeuchi, N., A. Selloni and E. Tosatti. *Physical Review Letters* 69 (1992): 648.

Takeuchi, N. (*see also* Selloni, A.)

Temnitschka, G. and R. Podloucky. *New Journal of Chemistry* (in print 1992).

Troyer, M. *Helvetica Physica Acta* 64 (1991): 700.

Tsunetsugu, H., M. Sigrist and K. Ueda. "On the Phase Diagram of the One-Dimensional Kondo Lattice Model." ETH-preprint (1992).

Tsunetsugu, H. (*see also* Troyer, M.; Ueda, K.)

Vittadini, A., A. Selloni, R. Car and M. Casarin. *Physical Review B* 46 (1992): 4348.

Vittadini, A. (*see also* Selloni, A.)

von Freyberg, B. and W. Braun. *Journal of Computational Chemistry* (in press 1992).

von Freyberg, B., T.J. Richmond and W. Braun. (submitted).

Ueda, K., H. Tsunetsugu and M. Sigrist. "Phase Diagram of the Kondo Lattice Model." In *Proceedings, SCES'92*, Sendai. September 7-11, 1992.

Ueda, K. (*see also* Tsunetsugu, H.)

Würtz, D. (*see* Assaad, F.F.)

Colloquia

Invited Speakers

BENISTON, Dr. Martin—ETH Zürich, Switzerland.
"Global Climate Change."

BHATT, Prof. Pramod Chandra P.—Indian Institute of Technology, Department of Computer Science and Engineering, New Dehli, India.
"Large-Scale Computing Applications in India: the Policy Perceptions."

DEGTYAREV, Prof. Lev—Keldysh Institute for Applied Mathematics, Moscow, CUI.
"Adaptive Grid Generation."

GIORGILLI, Dr. Antonio—Politecnico di Milano, Milano, Italy.
"Introduzione ai sistemi dinamici con applicazioni alla meccanica celeste."

GROSS, Prof. Thomas—School of Computer Science, Carnegie Mellon University, Pittsburgh, USA.
"Aspects of the iWARP Development."

HELLER, Moshe R.—Bi-National Technology Utilizing Simulation, Manno, Switzerland.
"ARINS: An Air-conditioning and Ventilation Simulation Engineering Tool."

SCHAAD, Dr. M. and Dr. Roland HENZI—Elektrowatt Ingenieurunternehmungen AG, Zürich, Switzerland.
"Project Idea ESNET-CSCS: Engineering and Science Network."

SCHUDEL, Peter E.—P.E.S. of Switzerland.
"Virtual Reality: Project Ticino."

SUCCI, Dr. Sauro—IBM Research Center, Rome, Italy.
"Lattice Boltzmann Method for CFD Problems."

WALLACE, Prof. David—Edinburgh Parallel Computing Centre, University of Edinburgh, UK.
"Massively Parallel Computing: Status, Industrial Impacts and Prospects."

CSCS Member Presentations

BERNASCONI, Andrea—"Le macchine vettoriali" CSCS [March 13, 1992].

BERNASCONI, Andrea—"Una trasformazione nello spazio delle fasi per il modello Coulombiano bidimensionale a una componente" Cerfim Locarno, Switzerland [November 1, 1992].

DECKER, Karsten—"Program and Application Development for Closely-Coupled Multicomputers" CSCS [June 11, 1992].

GRUBER, Ralf—"Parallel Machines in the 90's: Hardware and Software Trends" CSCS [May 7, 1992].

GRUBER, Ralf—"Thermonuclear Fusion: Energy of the Future?" CSCS [June 3, 1992].

GRUBER, Ralf—"Thermonuclear Fusion: Energy of the Future?" Research Center for Mathematics and Physics, Locarno, Switzerland [May 8, 1992].

GRUBER, Ralf—"Technological Applications at the Swiss Supercomputer Center." CATSUPERCOMP, Barcelona, Spain.

GRUBER, Ralf—"Simulation of Magnetic Fusion Devices." Public Conference on the Use of Supercomputers in Science and Industry, Monte Verita', Ascona, Switzerland [June 1-5, 1992].

MARIC, Djordje—"Electronic Structure of Hydrogen-Containing Defects in Semiconductors: Cluster Calculations" CSCS [February 19, 1992].

MARIC, Djordje—"A Presentation of CSCS: Three Examples of ongoing Supercomputing Projects of Zürich University." University of Zürich, Switzerland [December 9, 1992].

MEYER, Urs—"Schattenerzeugung in Ray-Tracing- und Radiosity-Verfahren." SCGA 12. Jahrestagung, Zürich-Oerlikon, Switzerland [June 17, 1992].

MEYER, Urs—"Presentation about CSCS and Graphics Lab." Institut für Polymere, Organische Chemie, ETH Zürich, Switzerland [September 25, 1992].

SCARONI, Fiorenzo—"The Supercomputer in Research and Development." Public Conference on the Use of Supercomputers in Science and Industry, Monte Verita', Ascona, Switzerland [June 1-5, 1992].

SCARONI, Fiorenzo—"Integration of Supercomputing Technology with an Open System Environment at CSCS." UNIX-Tage '92 bei DEC, Dübendorf, Switzerland [March 4, 1992].

SCHEIDEGGER, Alfred—"Japan's Leadership in Technology: from Medieval Times to the 20th Century." New Technology Week of "Ingenieure für Die Schweiz von Morgen" ABB, Baden, Switzerland [September 15, 1992].

TOMASSINI, Marco—"Parallel Computational Complexity and its Significance in Parallel Algorithm Design" CSCS [May 15, 1992].

TOMASSINI, Marco—"The Role of Massively Data-Parallel Computers in Large-Scale Molecular Dynamics Simulations." 4th International Conference on Computational Physics, Prague, Czechoslovakia [August 24-28, 1992].

TOMASSINI, Marco—"Moderne Architetture Parallele e Vettoriali per il Calcolo Scientifico." Chemical Department, University of Perugia, Italy [November 23-24, 1992].

CSCS Via Cantonale 6928 Manno Switzerland